Modelling the outbreak of infectious disease following mutation from a non-transmissible strain

Modelling the outbreak of infectious disease following mutation from a non-transmissible strain

C.Y. Chen[a], J.P. Ward[b], W.B. Xie[a]

[a] *Department of Applied Mathematics, National University of Kaohsiung, Kaohsiung, Taiwan*
[b] *Department of Mathematical Sciences, Loughborough University, Loughborough, U.K.*

Abstract

In-host mutation of a cross-species infectious disease to a form that is transmissible between humans has resulted with devastating global pandemics in the past. We use simple mathematical models to describe this process with the aim to better understand the emergence of an epidemic resulting from such a mutation and the extent of measures that are needed to control it. The feared outbreak of a human-human transmissible form of avian influenza leading to a global epidemic is the paradigm for this study. We extend the SIR approach to derive a deterministic and a stochastic formulation to describe the evolution of two classes of susceptible and infected states and a removed state, leading to a system of ordinary differential equations and a stochastic equivalent based on a Markov process. For the deterministic model, the contrasting timescale of the mutation process and disease infectiousness is exploited in two limits using asymptotic analysis in order to determine, in terms of the model parameters, necessary conditions for an epidemic to take place and timescales for the onset of the epidemic, the size and duration of the epidemic and the maximum level of the infected individuals at one time. Furthermore, the basic reproduction number R_0 is determined from asymptotic analysis of a distinguished limit. Comparisons between the deterministic and stochastic model demonstrate that stochasticity has little effect on most aspects of an epidemic, but does have significant impact on its onset particularly for smaller populations and lower mutation rates for representatively large populations. The deterministic model is extended to investigate a range of quarantine and vaccination programmes, whereby in the two asymptotic limits analysed, quantitative estimates on the outcomes and effectiveness of these control measures are established.

Keywords: Epidemic, mutation, mathematical models, differential equations, stochastic process, asymptotic analysis.

1. Introduction

Cross-species transmission of viruses from animals to human and their subsequent evolution have in the past led to epidemics some with disastrous results on a global scale. HIV/AIDS, severe acute respiratory syndrome (SARS), West Nile virus and the Spanish flu of 1918 are just a few examples [12, 29]. Viruses continue to present new threats, a recent example being the ebola outbreaks in West Africa (2014-2016, with 28616 known cases and 11310 deaths, as of June 2016) and in the Democratic Republic of the Congo (2018-, 56 cases and 25 deaths, as of early June 2018) [36]. Another example is the avian influenza, in particular the H5N1 virus which has been circulating since 1997 in parts of Asia and some regions of Africa with 860 confirmed cases of human infection (454 deaths) in the years between 2003 and 2018 [37]. This disease in its current state does not readily infect humans, but can spread rapidly amongst domesticated

birds with a mortality rate as high as 100% [1]. Human cases have resulted from direct or close contact with infected poultry (domesticated chickens, ducks and turkeys). The spread of avian influenza from an infected person to another has rarely been reported and the transmission has not been observed to continue beyond one person. All influenza viruses, however, have the ability to change and adapt. Past examples, such as the Spanish flu, have shown that this could result with a transmissible virus which can spread easily and directly to humans. Such an outbreak could develop into an epidemic on a global scale, potentially taking millions of lives. A better understanding of the dynamics of how events leading to an epidemic can help to control and eradicate the disease and to prevent an infectious disease from developing into an epidemic.

Viruses are highly prone to genetic mutation, influenza viruses being well-studied examples. Minor mutations may involve small changes to surface glycoproteins, resulting with a strain of the same viral subtype that can deceive the adaptive immune response, and reinfect a previously infected host. This kind of mutation is known as antigenic drift and leads to recurrent, often annual, outbreaks of an influenza subtype. More dramatic mutations leading to new viral subtypes are known as antigenic shifts, which can arise in at least two ways. The first way is known as reassortment in which influenza viruses of two different subtypes infect the same host simultaneously, whereby genetic material could be exchanged to form a new, viable virus. This is a feared possibility regarding individuals infected by both the human and avian form of influenza, leading to a transmissible form of the disease. The second involves direct or indirect introduction of an avian influenza virus into humans which subsequently adapt to the new host [28, 10]. The new virus subtype, with no antibodies against it present in the human body, will transmit easily from human to human, as a result, a global pandemic may occur.

Mutations of the highly pathogenic avian influenza virus from a non-transmissible form to one that is rapidly transmissible among humans is treated here as an antigenic shift and not a result of a sequence of antigenic drift events, and hence is modelled as a one-step process taking place within its human host. The indirect transmission of the mutated virus into humans via an intermediate host (e.g. pigs) is not considered here, the model developed, however, can be adopted to include an intermediate host without too much difficulty. The relative simplicity of the system we study enables a detailed analysis to be carried out, from which a number of key characteristics of an epidemic following disease mutation can be quantified in terms of the model's parameters.

Published models of avian flu have focused on the spread of disease between bird populations and farms [4, 21, 27, 34] and cross-species transmission between bird and human populations [7, 13, 15, 23]. In each of these studies their aim is to understand the dynamics of the disease and the effectiveness of measures to control in both bird and human populations. Each of the bird-human transmission models are extensions of the "standard" SIR compartmental formulation (Susceptibles-Infectives-Removed) for an *endemic disease* (i.e. natural birth and death processes are considered), whereby mutation to the human-human transmissible form emerges via antigenic shift in human hosts. The mutation events are assumed to have occurred either at a fixed rate [7, 13, 15] or as a spontaneous event at a given time point [23]. The core of the analysis investigates the stability of equilibria and establishing the basic reproduction numbers of the disease in the populations. In contrast to these studies, we analyse in this paper a model that describe the potential development of an *epidemic* of human-human transmission form of flu by focussing on the human population only, whereby bird-human transmission only occurs to a sub-population of humans (bird handlers) at a fixed rate (assuming an approximately fixed population of diseased birds). In common with the above mentioned avian flu models, we extend the SIR formulation and assume mutation is via antigenic shift in humans, however, we analyse

in much more detail the transient behaviour (e.g. timescales for epidemic outbreak, duration of epidemic) as well as the long-time dynamics. Moreover, a stochastic version of the model is investigated to assess the reliability of the predictions from a continuum model in a range of circumstances. We note that modelling epidemics using SIR based models has had a long history since the seminal work of Kermack and McKendrick in 1927 [18], including applications to influenza, sexually transmitted disease, the "Bombay plague" [25] and West Nile virus [35]. Amongst the mathematical extensions include more general infection rate kinetics [19], terms with time delays [16, 30], stochasticity [32, 33] and spatial spread [17]. We also note there are a number of epidemic models examining mutations and genetic drift (e.g. [5, 11, 22, 26]), many of which are more sophisticated than the proposed model, but at a cost at being more difficult to analyse.

In this paper we propose a simple deterministic model and a stochastic equivalent to describe in-host viral mutation of a cross-species disease that enables human-human transmission. Whilst the former model is expected to be mainly applicable to large populations, the slow mutation process suggests that stochasticity is important, particularly early in an epidemic. We analyse these models to determine the effects of parameters on a number of features of an epidemic (onset time, epidemic duration etc.), establishing the strengths and weaknesses of the two approaches. Furthermore, the deterministic model is extended to investigate potential measures in disease control. Though the model provides a general framework for in-host mutation more virulent forms of disease, we use the much feared avian flu scenario as a paradigm.

The paper is arranged as follows. In the next section, the mathematical model is derived to describe the spread of a bird-human transmissible virus, which can mutate into a human-human transmissible form. Only a fraction of the population is assumed to be at risk of the bird-human transmissible form, but the whole population is vulnerable to the mutated version. We carry out large-time (Section 3) and asymptotic (Section 4) analysis to obtain predictions, in terms of reduced model solutions, on the possible development of an epidemic. In Section 5 the effects of intervention by means of quarantine and vaccination are investigated. The stochastic version of the model is presented and analysed in Section 6 and we conclude with an overview of the result in Section 7.

2. Deterministic Model

The model proposed below aims to describe in-host mutation of a non-human-human transmissible to a human-human transmissible virus strain and its spread throughout a population. The population is assumed well mixed and of size ranging from $N = 10^5 - 10^9$, i.e. anywhere from large city to continental scale. Though the development of mutant viral forms may take years to develop, an epidemic may last just a few weeks; we assume over the timescale of interest the demographic turnover is negligible so that the total population remains constant. The entire population is broadly compartmentalised into susceptible, infective and recovered (or removed) classes and the populations vary continuously in time. In the case of avian flu, only a fraction of a population are exposed to birds who are themselves exposed to the bird-bird transmissible form of avian flu. We thus split the susceptible class into two, one class that are bird-handlers (mainly poultry farmers) at risk of catching flu directly from their birds and the other class who are not exposed to potentially diseased birds. We note, that this assumption has general application, for example, where sub-populations have different exposure to a non-human-human transmissible disease based on their activity or their geographical location. We will not be modelling bird populations explicitly and assume that their numbers are constant. Those infected

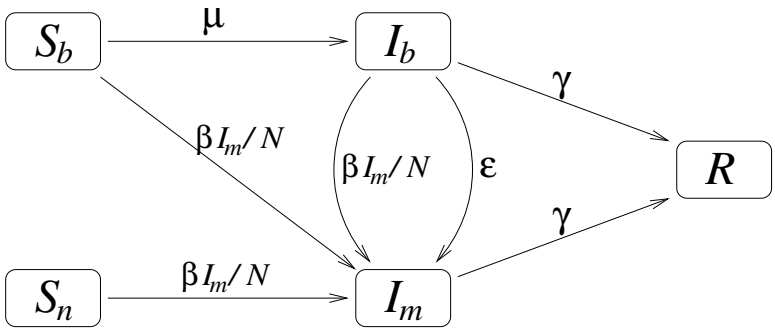

Figure 1: Schematic of the infection and mutation pathways used in the derivation of the model.

by the bird-human transmissible form of avian flu are not able to infect other susceptibles, unless the virus has mutated to a human-human transmissible form, thus two infected classes are assumed. To summarise, the total population is divided into five subclasses:

S_b : population of the bird-handlers at risk of catching avian flu from birds.

S_n : population of individuals not at risk of catching avian flu from birds.

I_b : population of infectives with only the non-mutated bird-human transmissible avian flu.

I_m : populations of infectives with the mutated, human-human transmissible avian flu.

R : population of those recovered/removed from either form of avian flu.

with S, I and R conventionally denote the susceptible, infective and removed/recovered. The variable R is the population who has survived or died from the disease; taking the mortality fraction to be η, then ηR is the number of deaths from the disease (currently $\eta \approx 0.53$ [37]). We note that we have assumed that recovery from one form of the flu leads to immunity against both forms.

The pathway summarising the interaction between the population classes is illustrated in Figure 1, and a summary of the modelling assumptions is as follows,

- The total population N is constant.
- Only the bird-handler class S_b can (spontaneously) catch avian flu from birds.
- Non-mutated avian flu cannot be transmitted from person to person.
- I_b becomes I_m through infection by I_m or through mutation of the virus.
- S_n, S_b and I_b can be infected by I_m.
- The two forms of flu are sufficiently similar for the removal rate to be the same.
- Once the infected I_m and I_b are recovered, they become immune to both forms.

The above assumptions do not distinguish between a person infected with a mutated form of the disease and one infected with both non-mutated and mutated form since the latter affects

the disease progress in the same way as the former does. Using these assumptions, the following system of ODEs is obtained:

$$\frac{dS_b}{dt} = -\mu S_b - \frac{\beta}{N} I_m S_b, \tag{2.1}$$

$$\frac{dS_n}{dt} = -\frac{\beta}{N} I_m S_n, \tag{2.2}$$

$$\frac{dI_b}{dt} = \mu S_b - \varepsilon I_b - \gamma I_b - \frac{\beta}{N} I_m I_b, \tag{2.3}$$

$$\frac{dI_m}{dt} = \frac{\beta}{N} I_m (S_b + S_n + I_b) - \gamma I_m + \varepsilon I_b, \tag{2.4}$$

$$\frac{dR}{dt} = \gamma (I_m + I_b), \tag{2.5}$$

where the sum of the populations is constant

$$N = S_n(t) + S_b(t) + I_m(t) + I_b(t) + R(t). \tag{2.6}$$

The rate constants in the system of the equations are

μ : disease infection rate constant from birds to humans,

β : infection rate constant of the human-human transmissible avian flu,

ε : mutation rate constant from I_b to I_m,

γ : recovery/removal rate constant for both I_m and I_b.

We note that although the disease in the bird population is not explicitly modelled, the proposed system (2.1)-(2.5) can be viewed as a limiting case of such a model. If the disease dynamics of the bird population occurs on a much faster timescale than the processes of bird-human transmission and disease mutation (e.g. as in [15]), then after a transient period the infected bird population will be close to steady-state (assumed stable) whilst human form of the disease continues to evolve. Since the infected bird population is effectively fixed in this scenario, the rate of bird-human transmission will be proportional to the susceptible bird-handler population, with μ being the constant of proportionality.

To close the system we suppose that initially, at $t = 0$, the first cases of the bird-human transmissible form of the disease arise; formally, the infection rate μ is defined to be $\mu = 0$ for $t < 0$ and $\mu > 0$ for $t \geq 0$. Consequently, we assume that initially there is nobody in the infected or recovered classes, hence

$$t = 0: \qquad S_n = s_0, \;\; S_b = N - s_0, \;\; I_b = I_m = R = 0,$$

where $s_0 \in [0, N)$ is the initial population of those not at risk of catching the bird-human transmissible form of the disease.

In contrast to most ordinary differential equation models in epidemiology, the disease is initiated by the bird-human transmission term μS_b in equations (2.1) and (2.3), rather than an assumed initial infected population. As a consequence, whilst $S_b > 0$, there is no disease-free state to determine the basic reproduction number R_0 using, for example, the next generation operator method. In this paper we will use the following definition,

Definition 2.1. The *basic reproduction number*, R_0, is defined as a formulation of the model parameters such that if $R_0 > 1$ then $\max_{t\in(0,\infty)} I_m/N = O(1)$, whilst if $R_0 < 1$ then $\max_{t\in(0,\infty)} I_m/N \ll 1$.

In the analysis of Section 4 and Appendix A the $O(1)$ term is in the context of a small parameter ε/γ, whereby in the limit $\varepsilon/\gamma \to 0$ a formula for R_0 is derived.

2.1. Non-dimensionalisation

In the analysis to follow it is convenient to non-dimensionalise the model using the rescalings

$$t = \hat{t}/\gamma, \quad S_b = N\hat{S}_b, \quad S_n = N\hat{S}_n, \quad I_m = N\hat{I}_m, \quad I_b = N\hat{I}_b, \quad R = N\hat{R}. \tag{2.7}$$

These rescalings imply that all the non-dimensional dependent variables represent population fractions of each of the classes and that removal/recovery of an infected individual occurs in $\hat{t} \sim 1$ time. The non-dimensional form of the rate constants are

$$\hat{\varepsilon} = \frac{\varepsilon}{\gamma}, \quad \hat{\mu} = \frac{\mu}{\gamma}, \quad \hat{\beta} = \frac{\beta}{\gamma} \quad \text{and} \quad \hat{s}_0 = \frac{s_0}{N}; \tag{2.8}$$

we expect that $\hat{\varepsilon} \ll 1$, reflects the fact that most individuals with the non-mutated form will be recovered or died before the virus strain has a chance to mutate to the transmissible form, and for the case of avian flu $\mu \ll 1$, as so few individuals (< 1000) have caught the disease in the last decade. It turns out in the analysis to follow that $\hat{\beta}$ is not necessarily equal to the basic reproduction number R_0, as is the case in the standard SIR model (discussed in Section 4.2). The hats will henceforth be dropped for brevity and the dimensionless system of equations are

$$\frac{dS_b}{dt} = -\mu S_b - \beta I_m S_b, \tag{2.9}$$

$$\frac{dS_n}{dt} = -\beta I_m S_n, \tag{2.10}$$

$$\frac{dI_b}{dt} = \mu S_b - \varepsilon I_b - I_b - \beta I_m I_b, \tag{2.11}$$

$$\frac{dI_m}{dt} = \beta I_m(S_b + S_n + I_b) - I_m + \varepsilon I_b, \tag{2.12}$$

$$\frac{dR}{dt} = I_m + I_b, \tag{2.13}$$

with $S_n + S_b + I_m + I_b + R = 1$ and the initial conditions are

$$t = 0: \qquad S_n = s_0, \quad S_b = 1 - s_0, \quad I_b = I_m = R = 0,$$

where $s_0 \in [0, 1)$.

3. Large-time analysis

It is clear in the way the model is constructed that all susceptibles in the bird-handler class will eventually be removed as $t \to \infty$ and that the only steady-state of the system belongs to the family of solutions

$$(S_b, S_n, I_b, I_m, R) = (0, S_\infty, 0, 0, R_\infty), \tag{3.1}$$

where $R_\infty = 1 - S_\infty$. The steady-state $S_\infty \in [0, 1)$ is the population of non-bird-handler suscetibles, S_n, as $t \to \infty$. The value of S_∞, as with the standard SIR model, is dependent on the initial conditions and is discussed further below. Linear stability analysis on this steady-state results with a Jacobian that has a zero eigenvalue, with all others being negative provided that

$$S_\infty \ < \ \frac{1}{\beta}, \tag{3.2}$$

thereby (3.1) is neutrally stable. By analogy to the standard SIR model, this results suggests that the basic reproduction number R_0 for this system is given by $R_0 \approx \beta$. This is true when the parameters μ and ε are $O(1)$ constants, whereby, the mutation happens sufficiently fast for the whole population to be vulnerable to the human-human transmissible form of the disease. However, as discussed in Section 4.2, R_0 will change as $\varepsilon \to 0$. Nevertheless, the inequality (3.2) suggests that in large time S_n will tend to a population S_∞ satisfying the inequality $0 \leq S_\infty \leq \min(1, 1/\beta)$. As expected, the fraction of susceptibles that remain following an epidemic will be reduced on increased virulence β.

One of the key aims of the modelling is to try to predict, in terms of the model parameters, the total mortality following a human-human transmissible disease epidemic, i.e. ηR_∞, recalling that η is the disease's mortality fraction. For the standard SIR model this is straightforward to do, resulting with R_∞ being the solution of an implicit equation [3, 24]. A similar approach can be used in the present model, though the details are more complicated. In the analysis below, we will establish a readily computable bound on S_∞, from which we can deduce bounds on R_∞.

Eliminating I_m using equations (2.9) and (2.10) leads to, on integration,

$$S_b \ = \ \frac{(1 - s_0)}{s_0}\, e^{-\mu t}\, S_n. \tag{3.3}$$

Eliminating I_m using (2.9) and (2.11) gives

$$\frac{1}{S_b}\frac{dS_b}{dt} - \frac{1}{I_b}\frac{dI_b}{dt} \ + \ \mu\, \frac{S_b}{I_b} = 1 + \varepsilon - \mu, \tag{3.4}$$

which can be solved and, following the substitution of (3.3), to get

$$I_b \ = \ \frac{\mu(1 - s_0)}{s_0(1 + \varepsilon - \mu)} \left(e^{-\mu t} - e^{-(1+\varepsilon)t}\right) S_n. \tag{3.5}$$

The case of $1 + \varepsilon - \mu = 0$ is not singular in the qualitative sense and leads to the solution $I_b = \mu(1 - s_0)te^{-\mu t}S_n/s_0$; this case does not produce any new behaviour of interest and will not be discussed further by assuming in what follows that $1 + \varepsilon - \mu \neq 0$. As a side note, the system (2.1)-(2.4) can be reduced to a nonlinear 2nd-order differential equation by using I_m from (2.10) and equations (3.3) and (3.5), namely

$$\frac{d^2S_n}{dt^2} - \frac{dS_n}{dt}\left(\frac{1}{S_n}\frac{dS_n}{dt} - 1 + \beta S_n\left(1 + \frac{1 - s_0}{s_0(1+\varepsilon-\mu)}\left((1 + \varepsilon)e^{-\mu t} - \mu e^{-(1+\varepsilon)t}\right)\right)\right) + \frac{\beta\mu\varepsilon(1 - s_0)}{s_0(1+\varepsilon-\mu)}\left(e^{-\mu t} - e^{-(1+\varepsilon)t}\right) S_n^2 \ = \ 0. \tag{3.6}$$

However, to determine the long time behaviour it is simpler to add equations (2.9)-(2.12) and substituting I_m from (2.10) to yield on integration,

$$S_n \ + \ S_b \ + \ I_b \ + \ I_m \ - \ 1 \ = \ \frac{1}{\beta}\ln\!\left(\frac{S_\infty}{s_0}\right) \ - \ \int_0^t I_b(z)\, dz.$$

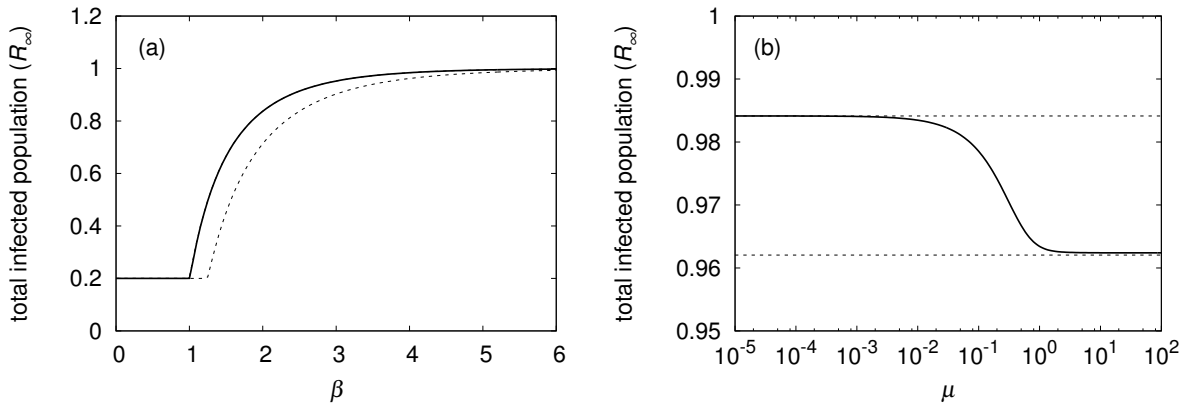

Figure 2: Plots of R_∞ (solid) and the upper and lower bounds determined from (3.12) (dashed lines). Plot (a) shows R_∞ against β (using $\mu = 10^{-4}, \varepsilon = 10^{-4}, s_0 = 0.8$) and (b) R_∞ against μ (using $\beta = 4, \varepsilon = 10^{-4}, s_0 = 0.8$). Note the R_∞ line is super-imposed over the upper bound line in the left-hand plot.

Substituting (3.1) and using (3.5) lead to the following equation for which S_∞ is a solution,

$$G(S_\infty, \Psi(S_n)) \;=\; \beta(1 - S_\infty) + \ln\left(\frac{S_\infty}{s_0}\right) - \;\frac{\beta\,(1 - s_0)}{s_0(1+\varepsilon)}\,\Psi(S_n) \;\;=\;\; 0, \tag{3.7}$$

where $\Psi(.)$ is the integral operator

$$\Psi(S_n) \;=\; \frac{\mu(1+\varepsilon)}{1+\varepsilon-\mu}\int_0^\infty S_n(z)\left(e^{-\mu z} - e^{-(1+\varepsilon)z}\right)dz, \tag{3.8}$$

which has been defined to have the property $\Psi(c) = c$ for constant c. In the standard SIR model, the steady-state value of S_n, say S_{SIR}, is the solution of $G(S_{SIR}, 0) = 0$, hence the integral term Ψ results from the additional assumptions in the current model.

Finding the solution S_∞ satisfying $G(S_\infty, \Psi(S_n))$ is not possible without full knowledge of the solution $S_n(t)$, however, an upper and lower bound can be determined. Viewing Ψ as a variable and S_∞ as a function of Ψ, we can deduce from (3.7) that

$$\frac{dS_\infty}{d\Psi} \;=\; \left(\frac{1}{S_\infty} - \beta\right)^{-1}\frac{\beta(1-s_0)}{s_0(1+\varepsilon)} \;>\; 0, \tag{3.9}$$

since $1/S_\infty - \beta > 0$ from (3.2). So the solution S_∞ of $G(S_\infty, \Psi) = 0$ increases on increasing Ψ. Moreover, $\Psi(S_n) \geq 0$ for any non-negative $S_n(t)$ since the bracketed term in the integral (3.8) has the same sign as $1 + \varepsilon - \mu$ (neglecting the case when this is zero). From (2.10), S_n is a monotonic decreasing functions, so $S_\infty \leq S_n(t) \leq s_0$, which means that $\Psi(S_n)$ is bounded by

$$S_\infty \;=\; \Psi(S_\infty) \;\;\leq\;\; \Psi(S_n) \;\leq\;\; \Psi(s_0) = s_0, \tag{3.10}$$

using the property of Ψ stated above. Using (3.9) and (3.10) the following bound on S_∞ can be deduced

$$S_{low} \;\leq\; S_\infty \;\leq\; S_{high}, \tag{3.11}$$

where constants S_{low} and S_{high} satisfy $G(S_{low}, S_{low}) = 0$ and $G(S_{high}, s_0) = 0$, respectively, both being straightforward to calculate numerically. Of more interest is the bound on R_∞, namely

$$R_{low} \;\leq\; R_\infty \;\leq\; R_{high}, \tag{3.12}$$

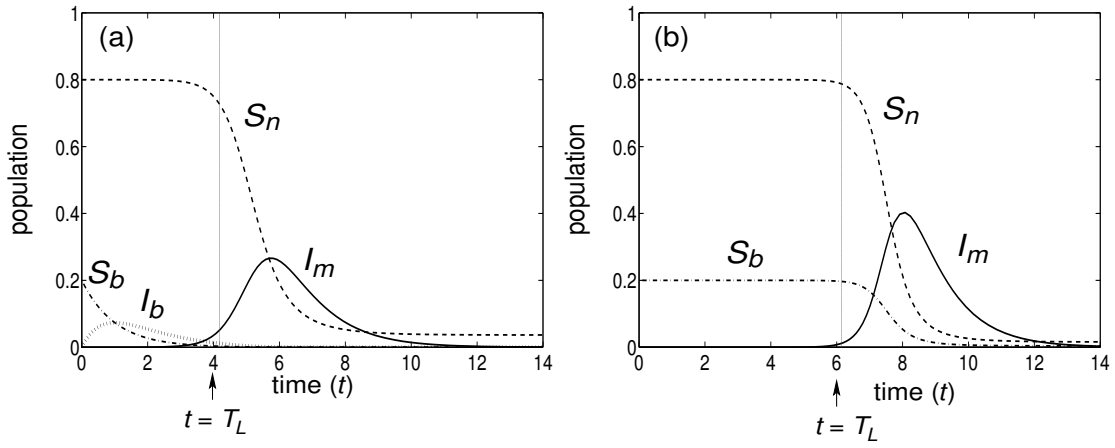

Figure 3: The evolution of S_b, S_n, I_b and I_m where (a) $\mu = 1$, $T_L = \ln(1/\varepsilon)/(\beta s_0 - 1)$ and (b) $\mu = 10^{-4}$, $T_L = \ln(1/\varepsilon\mu)/(\beta - 1)$ with $\beta = 4$, $\mu = 1$, $s_0 = 0.8$ and $\varepsilon = 10^{-4}$. Note that for case (b) I_b is negligibly small throughout the entire time.

where $R_{low} = 1 - S_{high}$ and $R_{high} = 1 - S_{low}$. Figure 2 shows plots of the bounds, given by (3.12), and numerically determined values of R_∞ against β and μ. The upper bound appears to provide a very good approximation of R_∞ for all values of β; this was found to be true for small μ, but as μ approaches $O(1)$, R_∞ tends to the lower bound. The reason for this is discussed in Section 4.2. The functions that determine the upper and lower bounds are independent of μ, hence these values are constant in the right-hand figure. As $\mu > 0$ increases, R_∞ tends smoothly from the upper to the lower bound, with the lower bound seeming to be a very good approximation from $\mu = O(1)$.

It is worth noting from (3.9) that $S_{SIR} < S_\infty$, which suggests that applying the standard SIR model to describe transmissible avian-flu spread may significantly over-predict the extent of an epidemic, particularly if $\beta \approx 1$.

4. Numerical results and asymptotic analysis

Figure 3 shows the evolution of the population fractions S_n, S_b, I_b and I_m using parameters $\beta = 4$, $s_0 = 0.8$ and $\varepsilon = 10^{-4}$, noting that the mutation rate ε is small in the simulations with two distinct cases of bird-human infection rate $\mu = 1$ and $\mu = 10^{-4}$. We observe that there is an initial time period ($t < T_L$), in which when $\mu = 10^{-4}$ the majority of the population is unaffected by the disease, whereas for $\mu = 1$ the susceptible bird-handlers, S_b, are steadily acquiring the bird-human transmissible form of the disease. At around the time indicated by the vertical line ($t = T_L$), the epidemic of the mutated transmissible form begins affecting the whole population. One of the interesting features in these simulations is this apparent time lag before the onset of the epidemic, moreover the occurrence of the bird-human transmissible form appears to be negligible during the epidemic. We note increasing ε moves the $t = T_L$ line to the left, whereby for $\varepsilon = O(1)$ there is no delay in the emergence of the mutated flu epidemic.

We investigated the model in two biologically relevant cases using singular perturbation theory, namely (1) $\varepsilon \to 0$ and $\mu \to 0$ and (2) $\varepsilon \to 0$ and $\mu = O(1)$. Since case (1) is most relevant for avian flu, whereby the rates of bird-human disease transmission and mutation are very low, we present the analysis in some detail in Section 4.1, whilst that for case (2) is briefly summarised in Section 4.2. The method used provides a systematic process by which

the solutions of the model are separated as a sequence of timescales, within which the dominant processes are identified and represented by reduced versions of the equations. The aim is to determine, in terms of the model's parameters, key quantities that characterise an epidemic, namely

- the epidemic's basic reproduction number R_0, as defined just before Section 2.1.
- the timescale for the onset of the epidemic T_L following the first cases of the bird-human transmissible form of the disease.
- the maximum level of infected individuals at one time I_{max}.
- the fraction of the population to have contracted the disease given by the final size of the removed class R_∞.
- the duration of the epidemic T_σ, defined to be the time in which the fraction of population who are infected by the mutated disease, I_m, is above a threshold value σ.

The analysis of Section 3 goes some way to answer the fourth quantity, however, the analysis below will give good approximations to the model predictions for all five quantities in the cases of $\varepsilon, \mu \to 0$, as demonstrated in the next section, and $\varepsilon \to 0$ and $\mu = O(1)$.

4.1. The case $\varepsilon \ll 1$ and $\mu \ll 1$

As demonstrated in the numerical solutions shown in Figure 3, the low rates of infection $\mu \ll 1$ and mutation $\varepsilon \ll 1$ will result in an initial phase of low epidemiological activity, before the epidemic erupts and dies away. These phases will be made explicit by the analysis below. The first phase involves the equilibration in population of those infected by the bird-human transmissible form of avian flu over an $t = O(1)$ timescale. We will focus mainly on the leading order solutions of the variables in each timescale, which enables ε and μ to be independently small with the formal restriction of $\ln(1/\varepsilon) \ll 1/\mu$. This restriction states that the timescale for a mutation event $(1/\varepsilon)$ is much less than the exponential of the timescale for cross-species transmission $(e^{1/\mu})$ and arises from the time at which the solutions of the first timescale breakdown (see Section 4.1.1). The analysis for the case $\ln(1/\varepsilon) \gg 1/\mu$ follows that of the $\varepsilon \to 0$ and $\mu = O(1)$ limit summarised in Section 4.2 and the distinguishing features of these two limiting cases merge when $\ln(1/\varepsilon) \sim 1/\mu$ (analysed in Appendix A to determine an expression for R_0). We note, in order to distinguish variables for particular timescales, different superscript symbols are used.

4.1.1. $t = O(1)$

This timescale captures the initial phase of avian flu contraction from birds, though the fraction that acquires the disease is very small (size $O(\mu)$). Cases of the mutant form are relatively negligible (size $O(\varepsilon\mu)$). Denoting all variables in this timescale with a superscript "$*$", the appropriate rescalings are

$$t = t^*, \quad S_b = S_b^*, \quad S_n = S_n^*, \quad I_b = \mu I_b^*, \quad I_m = \varepsilon\mu I_m^*,$$

which leads to the system

$$\frac{dS_b^*}{dt^*} = -\mu S_b^* - \varepsilon\mu\,\beta I_m^* S_b^*, \tag{4.1}$$

$$\frac{dS_n^*}{dt^*} = -\varepsilon\mu\,\beta I_m^* S_n^*, \tag{4.2}$$

$$\frac{dI_b^*}{dt^*} = S_b^* - \varepsilon I_b^* - \varepsilon\mu\,\beta I_m^* I_b^* - I_b^*, \tag{4.3}$$

$$\frac{dI_m^*}{dt^*} = I_b^* + \beta I_m^*(S_b^* + S_n^* + \mu I_b^*) - I_m^*, \tag{4.4}$$

with $R^* \sim O(\mu)$, subject to $S_b^*(0) = 1-s_0, S_n^*(0) = s_0, I_b^*(0) = 0$ and $I_m^*(0) = 0$.

Formally, we write each dependent variable as a power series expansion, e.g. $S_b \sim S_{b_0} + \varepsilon S_{b_1} + \mu S_{b_2} + ...$, substitute them into the system of differential equations, equate the terms with the same powers of ε and μ and solve the resulting equations. Doing this we obtain the following leading approximations,

$$\begin{aligned}
S_b^* &\sim 1 - s_0 - \mu\,(1-s_0)\,t^* + \mu^2\,(1-s_0)\,\frac{t^{*2}}{2} \\
&\qquad - \varepsilon\mu\,(1-s_0)\left(\frac{1-s_0}{(\beta-1)^2}e^{(\beta-1)t^*} - (1-s_0)\left(e^{-t^*} + \frac{\beta}{\beta-1}\left(t^* - \frac{\beta-2}{\beta-1}\right)\right)\right), \\
S_n^* &\sim s_0 - \varepsilon\mu\, s_0(1-s_0)\left(\frac{1}{(\beta-1)^2}e^{(\beta-1)t^*} - e^{-t^*} - \frac{\beta}{\beta-1}\left(t^* - \frac{\beta-2}{\beta-1}\right)\right), \\
I_b^* &\sim (1-s_0)(1-e^{-t^*}), \\
I_m^* &\sim \frac{(1-s_0)}{\beta(\beta-1)}(e^{(\beta-1)t^*} - 1) + \frac{(1-s_0)}{\beta}\left(e^{-t^*} - 1\right),
\end{aligned}$$

up to $O(\varepsilon^a\mu^b)$ where $a+b \le 2$. The expansions show that initially the susceptible populations are mostly unaffected by both flu strains, with a fraction $O(\mu)$ bird-handlers and $O(\varepsilon\mu)$ non-bird-handlers infected. We note that the carriers of the human-human transmissible form of the disease I_m^* will grow exponentially if $\beta > 1$; this indicates that $R_0 \sim \beta$ in the combined limits of $\varepsilon \to 0$ and $\mu \to 0$. For $\beta > 1$, these expansions are valid whilst the incidence rate of catching the mutated form of the disease is significantly less than that of the bird-human transmissible form. Under the restriction of $\ln(1/\varepsilon) \ll 1/\mu$, these solutions breakdown when $\varepsilon\mu\beta = O(\mu)$ in equation (4.1), whereby the rates of obtaining the two forms become approximately the same. More precisely, in large time $I_m^* \sim A\,e^{(\beta-1)t^*}$, for constant $A = (1-s_0)/\beta(\beta-1)$, implies that breakdown occurs at $t^* \sim \ln(1/\varepsilon)/(\beta-1)$ as $\varepsilon \to 0$, leading to a new timescale of events in which human-human transmission begins to be the dominant means of propagating the mutated form of the disease. We note that if $\ln(1/\varepsilon) \gg 1/\mu$ the solutions breakdown at $t^* = O(1/\mu)$ as $dS_b^*/dt = O(1)$ at leading order, so the S_b population noticeably drops before the human-human transmission takes noticeable effect (we will not discuss this case further). The matching conditions for the next timescale's solutions are

$$\begin{aligned}
S_b^* \sim 1-s_0-\mu(1-s_0)t^* - \varepsilon\mu\,\frac{(1-s_0)^2}{(\beta-1)^2}e^{(\beta-1)t^*}, \quad S_n^* \sim s_0 - \varepsilon\mu\,\frac{s_0(1-s_0)}{(\beta-1)^2}e^{(\beta-1)t^*}, \\
I_b^* \sim (1-s_0), \quad I_m^* \sim \frac{(1-s_0)}{\beta(\beta-1)}e^{(\beta-1)t^*},
\end{aligned} \tag{4.5}$$

as $t^* \to \infty$.

For the relatively trivial case of $\beta < 1$, in large time the level of both forms of the disease reaches a maximum, namely $I_b^* \sim (1-s_0)$ and $I_m^* \sim (1-s_0)/(1-\beta)$ (i.e. $I_b \to O(\mu)$ and $I_m \to O(\varepsilon\mu)$ constant). In a timescale of $t = O(1/\mu)$ the balance in the expansions breaks down

leading to the second timescale of importance, in which $S_n \sim s_0 - O(\varepsilon)$ and $S_b \sim (1-s_0)e^{-t/\mu}$. Eventually every member of bird-handler class will be infected by the bird-bird transmissible form, but never sufficiently for the mutated form to ever talk hold. Here, $S_n \sim s_0$ and $S_b \to 0$ as $t \to \infty$.

The $\beta < 1$ case will not be discussed further and we will now focus on the $\beta > 1$.

4.1.2. $t = \ln(1/\varepsilon)/(\beta-1) + O(1)$

This timescale represents the phase in which contraction of the human-human transmissible form becomes the dominant means of catching the disease. Using the superscript "†" to denote the variables in this timescale, we write

$$t = \frac{\ln(1/\varepsilon)}{\beta-1} + t^\dagger, \quad S_b = S_b^\dagger, \quad S_n = S_n^\dagger, \quad I_b = \mu I_b^\dagger, \quad I_m = \mu I_m^\dagger,$$

noting that I_m is now $O(\mu)$. The rescaled equations are

$$\frac{dS_b^\dagger}{dt^\dagger} = -\mu\, S_b^\dagger - \mu\,\beta I_m^\dagger S_b^\dagger, \tag{4.6}$$

$$\frac{dS_n^\dagger}{dt^\dagger} = -\mu\,\beta I_m^\dagger S_n^\dagger, \tag{4.7}$$

$$\frac{dI_b^\dagger}{dt^\dagger} = S_b^\dagger - \varepsilon I_b^\dagger - \mu\,\beta I_m^\dagger I_b^\dagger - I_b^\dagger, \tag{4.8}$$

$$\frac{dI_m^\dagger}{dt^\dagger} = \varepsilon I_b^\dagger + \beta I_m^\dagger (S_b^\dagger + S_n^\dagger + \mu I_b^\dagger) - I_m^\dagger. \tag{4.9}$$

We note in contrast to the previous timescale, that the leading-order contribution to the human-human transmissible class $I_m^\dagger$ is now from infection of susceptible individuals rather than mutation from $I_b^\dagger$. The key leading terms in the expansion of this system, using the matching conditions (4.5) as $t^\dagger \to -\infty$, are

$$\begin{aligned}
S_b^\dagger &\sim 1-s_0 - \mu\left(\frac{(1-s_0)^2}{(\beta-1)^2}e^{(\beta-1)t^\dagger} + (1-s_0)t^\dagger\right),\\
S_n^\dagger &\sim s_0 - \mu\,\frac{s_0(1-s_0)}{(\beta-1)^2}e^{(\beta-1)t^\dagger},\\
I_b^\dagger &\sim 1-s_0,\\
I_m^\dagger &\sim \frac{(1-s_0)}{\beta(\beta-1)}e^{(\beta-1)t^\dagger},
\end{aligned}$$

as $\varepsilon, \mu \to 0$. In time the spread of the human-human transmissible form of the disease will become dominant and an epidemic will ensue. This will occur when $I_m^\dagger = O(1/\mu)$ (i.e. $I_m = O(1)$) in a timescale $t^\dagger = \ln(1/\mu)/(\beta-1)$, whereby the transmission rates will becomes O(1) and the expansions for this timescale are no longer valid. For matching with the next timescale solutions, we have

$$\begin{gathered}
S_b^\dagger \sim (1-s_0) - \mu\frac{(1-s_0)^2}{(\beta-1)^2}e^{(\beta-1)t^\dagger}, \quad S_n^\dagger \sim s_0 - \mu\,\frac{s_0(1-s_0)}{(\beta-1)^2}e^{(\beta-1)t^\dagger},\\
I_b^\dagger \sim 1-s_0, \quad I_m^\dagger \sim \frac{(1-s_0)}{\beta(\beta-1)}e^{(\beta-1)t^\dagger},
\end{gathered} \tag{4.10}$$

as $t^\dagger \to \infty$.

4.1.3. $t = \ln(1/\varepsilon\mu)/(\beta-1) + O(1)$

This timescale represents the epidemic phase of the disease in which, for a time, the fraction of infected individuals becomes $O(1)$. Denoting the variables for this timescale with the superscript "‡", we write

$$t \;=\; \frac{\ln(1/\varepsilon\mu)}{\beta-1} + t^{\ddagger}, \quad S_b \;=\; S_b^{\ddagger}, \quad S_n \;=\; S_n^{\ddagger}, \quad I_b \;=\; \mu I_b^{\ddagger}, \quad I_m \;=\; I_m^{\ddagger},$$

which gives

$$\begin{aligned}
\frac{dS_b^{\ddagger}}{dt^{\ddagger}} &= -\mu S_b^{\ddagger} - \beta I_m^{\ddagger} S_b^{\ddagger}, && (4.11)\\
\frac{dS_n^{\ddagger}}{dt^{\ddagger}} &= -\beta I_m^{\ddagger} S_n^{\ddagger}, && (4.12)\\
\frac{dI_b^{\ddagger}}{dt^{\ddagger}} &= S_b^{\ddagger} - \varepsilon I_b^{\ddagger} - \beta I_m^{\ddagger} I_b^{\ddagger} - I_b^{\ddagger}, && (4.13)\\
\frac{dI_m^{\ddagger}}{dt^{\ddagger}} &= \varepsilon\mu\, I_b^{\ddagger} + \beta I_m^{\ddagger}(S_b^{\ddagger} + S_n^{\ddagger} + \mu I_b^{\ddagger}) - I_m^{\ddagger}. && (4.14)
\end{aligned}$$

We note that in this timescale $I_b^{\ddagger}$ decouples from the system at leading order. Defining $S^{\ddagger} = S_b^{\ddagger} + S_n^{\ddagger}$, then the leading terms $S_0^{\ddagger}$ and $I_{m0}^{\ddagger}$ of the series expansions for $S^{\ddagger}$ and $I_m^{\ddagger}$, respectively, satisfy the classic SIR model,

$$\begin{aligned}
\frac{dS_0^{\ddagger}}{dt^{\ddagger}} &= -\beta I_{m0}^{\ddagger} S_0^{\ddagger}, && (4.15)\\
\frac{dI_{m0}^{\ddagger}}{dt^{\ddagger}} &= \beta I_{m0}^{\ddagger} S_0^{\ddagger} - I_{m0}^{\ddagger}, && (4.16)
\end{aligned}$$

subject to the conditions $S_0^{\ddagger} \to 1^-$ and $I_{m0}^{\ddagger} \to 0^+$ as $t^{\ddagger} \to -\infty$, using (4.10). Solving this system we get

$$I_{m0}^{\ddagger} \;=\; (1 - S_0^{\ddagger}) \;+\; \frac{1}{\beta}\ln\left(S_0^{\ddagger}\right). \qquad (4.17)$$

Since $dI_{m0}^{\ddagger}/dt = 0$ implies $S_0^{\ddagger} = 1/\beta$, then the leading-order maximum extent of the epidemic is given by $I_{max} = (\beta - 1 - \ln(\beta))/\beta$. Using the same approach, as described in Appendix B, the following estimate for the duration T_σ of the epidemic can be determined

$$T_\sigma \;\sim\; \left(1 + \frac{1}{\beta}\right)\ln(1/\sigma), \qquad (4.18)$$

as $\beta \to \infty$, recalling that the epidemic is "defined" to be when $I_{m_0}^{\ddagger} > \sigma$. As $t^{\ddagger} \to \infty$, the epidemic declines and $I_{m_0}^{\ddagger} \to 0$, then $S_0^{\ddagger}$ tends to a constant, $S_\infty^{\ddagger}$ say, given by

$$1 - S_\infty^{\ddagger} \;+\; \frac{1}{\beta}\ln\left(S_\infty^{\ddagger}\right) \;=\; 0. \qquad (4.19)$$

Since the human-human transmissible form of the disease does not distinguish between the two susceptible classes, it follows that $S_n^{\ddagger} \sim s_0 S_\infty^{\ddagger}$ and $S_b^{\ddagger} \sim (1-s_0)S_\infty^{\ddagger}$ as $t^{\ddagger} \to \infty$.

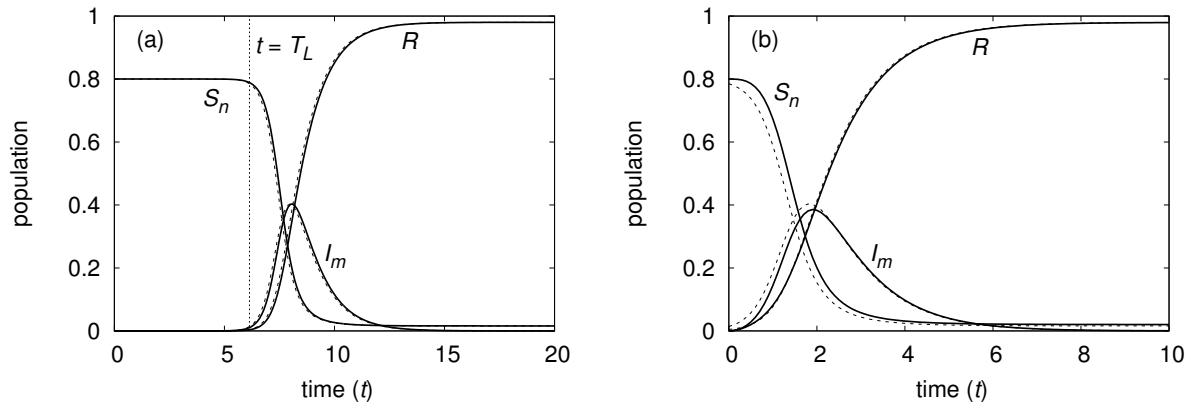

Figure 4: Comparison of numerical (solid) and the asymptotic approximations (dashed) presented in Section 4.1.3 for (a) $\varepsilon = \mu = 10^{-4}$ and (b) $\varepsilon = \mu = 1$. The dotted line in plot (a) shows $t = T_L = \ln(1/\varepsilon\mu)/(\beta - 1)$. The other parameters are $\beta = 4$ and $s_0 = 0.8$.

Figure 4 compares the numerical solutions for S_n, I_m and R (solid lines) with the leading order asymptotic approximations $S_n^\ddagger, I_m^\ddagger$ and $R^\ddagger = 1 - S_0^\ddagger - I_m^\ddagger$ (dashed lines). Here, equation (4.15) is solved numerically on substitution of (4.17) for $I_m^\ddagger$, using initial conditions derived by matching with (4.10) as $t^\ddagger \to -\infty$, namely at $t^\ddagger = -T < 0$ we impose $S_0^\ddagger(-T) = 1 - (1 - s_0)e^{-(\beta-1)T}/(\beta - 1)^2$ for suitably large T ($T = 10$ in the figures). As to be expected there is excellent agreement for $\varepsilon = \mu = 10^{-4}$ (fig. (a)), since both "small' parameters are very small, however, agreement continues to be good well beyond the expected range of validity as shown for $\varepsilon = \mu = 1$ (fig. (b)). The predicted epidemic onset time $t = T_L = \ln(1/\varepsilon\mu)/(\beta - 1)$ (dotted line in fig. (a)) also agrees well with solutions of the full problem.

The analysis is not quite complete as the balance on this timescale breaks down when the epidemic declines to the point when $I_m = O(\mu)$. Here, the infection rates of the S_b class by both forms of the disease are once again in balance; the appropriate system for this fourth timescale is the same as (4.6)-(4.9). The timescale at which $I_m^\ddagger = O(\mu)$ depends on β as well as ε; for example, in the limit $\beta \to \infty$ it occurs when $t^\ddagger = O(\ln(1/\mu))$. The leading order behaviour has $S_b \to 0, I_b \to 0, I_m \to 0$ and, the result of note in this new timescale, $S_n \sim s_0 S_\infty^\ddagger$ as $t \to \infty$. From (4.19), the total fraction of the population that will get either form of the disease satisfies $R_\infty \sim R_\infty^\ddagger = 1 - s_0 S_\infty^\ddagger$, where $R_\infty^\ddagger$ is given by

$$F(R_\infty^\ddagger, \beta) = 0,$$

and

$$F(R, R_0) \;=\; 1 - \frac{1-R}{s_0} \;+\; \frac{1}{R_0} \ln\left(\frac{1-R}{s_0}\right); \tag{4.20}$$

here, R_0 is the basic reproduction number, see Section 4.2. It is straightforward to show that $dR_\infty^\ddagger/ds_0 > 0$, so the fraction that will become infected increases with s_0. Furthermore, (4.20) has the following behaviour in two limits of β

$$\begin{aligned} \beta \sim 1 \qquad & R_\infty \;\sim\; 1 - s_0 + 2s_0(\beta - 1) - \frac{8s_0}{3}(\beta - 1)^2, \\ 1 \ll \beta \qquad & R_\infty \;\sim\; 1 - s_0 e^{-\beta} - s_0 \beta e^{-2\beta}, \end{aligned}$$

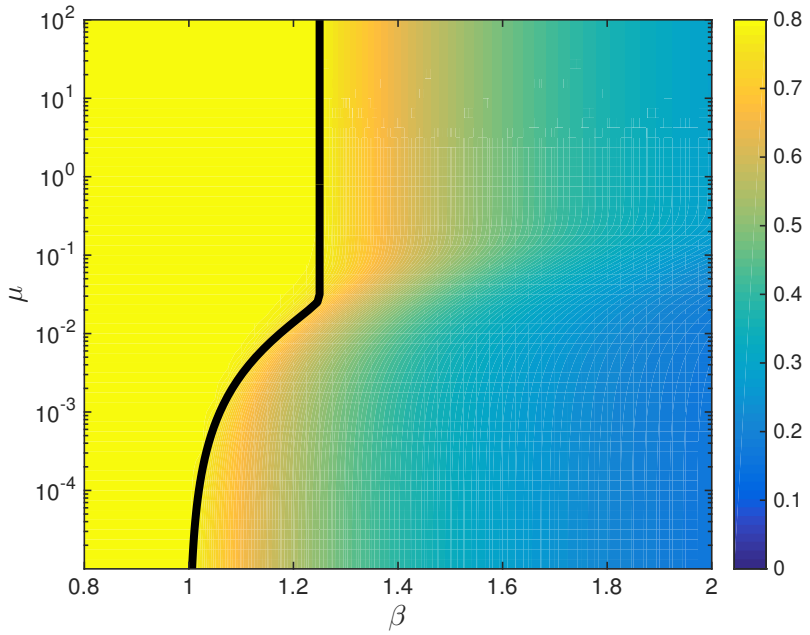

Figure 5: Heat map of S_∞ in $\beta - \mu$ space and the approximate position of $R_0 = 1$ (solid line) as given by equation (4.21). The other parameters are $\varepsilon = 10^{-4}$ and $s_0 = 0.8$.

In the first case, the effects of the human-human transmissible form is second order, with the contribution to the R class being from the infection of the S_b by the non-tranmissible form. For the highly infectious case, only an exponentially small fraction of the population avoids catching the disease.

Equation (4.20) is the same as that for $R_{high} = 1 - S_{low}$ in Section 3, i.e. $R_\infty^\ddagger = R_{high}$. Thus, in the limit $\varepsilon \to 0$ and $\mu \to 0$, the fraction of the population that acquires the disease is $R_\infty \sim R_{high}$, which is in agreement with the right plot of Figure 2 as $\mu \to 0$.

4.2. Summary of the asymptotic analysis

In addition to the $\varepsilon, \mu \ll 1$ limit, we used the same approach to examine the cases (1) $\varepsilon \to 0$ and $\mu = O(1)$ (details not shown) and (2) the distinguished limit $\mu \sim 1/\ln(1/\varepsilon)$ as $\varepsilon \to 0$ to determine an expression for R_0 (Appendix A). Much of the singular perturbation analysis for these limits follows exactly the same path as the above and we omit for brevity the details for case (1), and present a partially complete analysis for case (2) in Appendix A. In case (1), the non-mutated form of the disease readily infects the exposed portion of the susceptible population (though not relevant to avian flu, it may be applicable to other diseases). A notable feature for this case is the exposed portion of the population (i.e. the S_b class) is infected rapidly by the non-transmissible form in comparison to disease mutation, the effective population that is vulnerable to the mutated form are those that remain (i.e. the S_n class); consequently, the effective reproduction number for this new limit is $R_0 \sim \beta s_0$. This value of R_0 and that of $R_0 \sim \beta$ derived in Section 4.1.1 is bridged by case (2), where in Appendix A it is determined to

Epidemilogical features	$\varepsilon \to 0,\ \mu = O(1)$	$\varepsilon \to 0,\ \mu \to 0$
Basic reproduction number R_0	βs_0	β
Epidemic lag time T_L	$\frac{1}{\beta s_0 - 1} \ln(\frac{1}{\varepsilon})$	$\frac{1}{\beta - 1} \ln(\frac{1}{\varepsilon \mu})$
Maximum infected fraction I_{max}	$s_0 - \frac{1}{\beta} + \frac{1}{\beta} \ln(\frac{1}{\beta s_0})$	$1 - \frac{1}{\beta} + \frac{1}{\beta} \ln(\frac{1}{\beta})$
Epidemic Duration T_σ $(\beta \to \infty)$	$(1 + \frac{1}{\beta s_0^*}) \ln(\frac{s_0^*}{\sigma})$	$(1 + \frac{1}{\beta}) \ln(\frac{1}{\sigma})$
Infected Fraction R_∞	$F(R_\infty, \beta s_0) = 0$	$F(R_\infty, \beta) = 0$

Table 1: Table summarising estimates of the key characteristic quantities for an epidemic from the human-human transmissible form of the disease, in terms of the model parameters, as predicted by the model from the analysis in Sections 4.1 and from the equivalent analysis for $\varepsilon \to 0$ and $\mu = O(1)$. If $\beta \ll \ln(1/\varepsilon)$ as $\beta \to \infty$ then $s_0^* = s_0$, otherwise $s_0^* \approx 1$ is a good approximation (see Appendix B). The function $F(.,.)$ is defined in equation (4.20).

be

$$R_0 \;=\; \begin{cases} \beta \;-\; (1 - \beta s_0)\, \ln\left(\dfrac{\beta(1 - s_0)}{1 - \beta s_0}\right) \;-\; \mu \ln(1/\varepsilon) & \mu \;<\; (s_0^{-1} - 1)/\ln(1/\varepsilon), \\ \beta s_0 & \mu \;\geq\; (s_0^{-1} - 1)/\ln(1/\varepsilon), \end{cases} \tag{4.21}$$

in the limit $\varepsilon \to 0$. Here on $R_0 = 1$, we obtain $\beta = 1$ for $\mu \to 0$ and $\beta = 1/s_0$ for $\mu = O(1)$ as expected from the analysis of Section 4.1 and for case (1). Figure 5 shows a heat map of the converged fraction of susceptibles S_∞ as $t \to \infty$ for $\beta \in [0.8, 2]$ and $\mu \in [10^{-5}, 10^2]$. As expected to the left of the diagram $S_\infty \sim s_0$ and drops down as β increases passed the solid line. The solid line is the plot of equation (4.21) and tracks the edge where $S_\infty \sim s_0$ remarkably well considering the estimate is only logarithmically accurate. In what follows we will focus our discussion on the two principle limits (i) $\varepsilon, \mu \to 0$ and (ii) $\varepsilon \to 0$ and $\mu = O(1)$, and not discuss the distinguish limit further.

The asymptotic analysis of the model equations (2.9)-(2.13) enables the estimation of other key quantities that characterise epidemics in terms of the parameters using relatively simple formula; these are presented for the two principle limits in Table 1. Both these limits produces results which are qualitatively similar, but the details are slightly different. The main predictions of the analysis are

- The basic reproduction number R_0 given by (4.21) differs in the two limits due to the division in population classes of the susceptibles s_0. The analysis shows that this is due to the timescales and which form of the diseases each of the susceptible classes becomes infected by. For $\mu = O(1)$, members of the S_b class are infected more by the bird-human transmissible form, and consequently have all moved to the R class, to leading order, by the time the epidemic of the human-human transmissible form takes hold. For $\mu \ll 1$, nearly the whole population is susceptible at the onset of the epidemic.

- There will be a significant time lag from when the bird-human transmissible has reached its apparent peak, before the onset of the epidemic of the human-human transmissible form. This lag phase is lengthened by decreased mutation and infection rates, becoming infinite as $R_0 \to 1$. These results are demonstrated in Figure 6, showing the effect $R_0 = \beta$ on the evolution of I_m (left) and S_n (right).

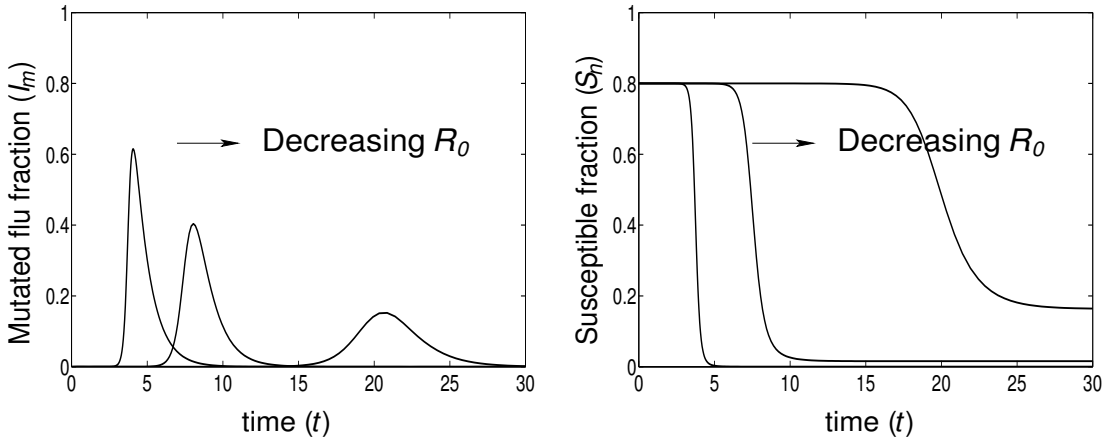

Figure 6: The evolution of I_m and S_n for $R_0 = \beta = 2, 4, 8$ and $\varepsilon = \mu = 10^{-4}$ and $s_0 = 0.8$.

- During the epidemic, the maximum infected fraction and epidemic duration increase with s_0 (see Table 1). This indicates the perhaps unintuitive result that if the bird-human transmissible is less infectious (smaller μ) then the epidemic from the human–human transmissible form will be worse.

- The leading order system that results during the epidemic timescale, equations (4.15) and (4.16), is the classic SIR (Susceptible-Infectious-Removed) model; this is true for $\varepsilon \ll 1$ and $\mu = O(1)$ case as well, though $S_0^{\ddagger}$ is replaced with $S_{n_0}^{\ddagger}$. The usual discussion of the SIR model involves a finite initial number of infectives, $I_0 > 0$ say, whilst in contrast the current system involves an infinitesimally small initial state, i.e. $I_0 \to 0^+$. This means that the extent of the epidemic corresponds to the least severe case of that predicted by the standard SIR model.

- The upper and lower bounds derived for R_∞ in Section 3 correspond to equation (4.20) for $\mu \ll 1$ and $\mu = O(1)$ cases, respectively, as $\varepsilon \to 0$. This explains why the R_∞ is nearly equal to the upper bound solutions in the left of Figure 2.

The first two points offer some insights into how the disease or epidemic could be managed. Though the mutation rate cannot be altered, the infection rate β and the fraction of susceptible population could be manipulated by quarantining and vaccination programmes. This is discussed in the next section.

5. Eradication and control: quarantine and vaccination

The analysis of the previous section showed that having some form of direct or indirect control over the infection rates β and μ and the population fraction of suseptibles s_0, could significantly reduce the impact of the disease. In this section, we discuss simple extensions to the model to investigate the possible outcomes of a range of quarantine and vaccination measures. We note that similar studies were undertaken on the avian flu models using numerical simulation [7] and sensitivity analysis [23]. Here, we are able to derive analytical expressions to assess the efficacy of treatment strategies.

5.1. Quarantine

It is clear that quarantining will help reduce the impact of the disease, so the aim here is to quantify its effects. We model quarantining by simply removing members of the infected class at a rate proportional to the fraction of infected individuals. Equations (2.1) and (2.2) are unchanged by this assumption and equations (2.3) - (2.5) become

$$\frac{dI_b}{dt} = \mu S_b - \varepsilon I_b - \gamma I_b - qI_b - \frac{\beta}{N} I_m I_b, \tag{5.1}$$

$$\frac{dI_m}{dt} = \frac{\beta}{N} I_m (S_b + S_n + I_b) + \varepsilon I_b - \gamma I_m - qI_m, \tag{5.2}$$

$$\frac{dR}{dt} = (\gamma + q)(I_m + I_b), \tag{5.3}$$

where q is the quarantining rate constant. Equation (5.2) implies that the average timescale an infective individual is infectious to others is reduced from $1/\gamma$ to $1/(\gamma+q)$. Non-dimensionalising using the rescalings (2.7) and (2.8) and writing $\hat{q} = q/\gamma$ leads to the obvious modification of (5.1)-(5.3), (the hat being dropped in what follows). Using the analytical approaches described in (4.1) and the equivalent for the $\mu = O(1)$ case, we deduce the following

$\varepsilon \ll 1$ and $\mu = O(1)$. The basic reproduction number becomes $R_0 \sim \beta s_0 - q$ and, for $R_0 > 1$, the epidemic time lag T_L is approximately $\ln(1/\varepsilon)/(\beta s_0 - 1 - q)$.

$\varepsilon \ll 1$ and $\mu \ll 1$. Here, $R_0 \sim \beta - q$ and, for $R_0 > 1$, the time lag T_L is approximately $\ln(1/\varepsilon\mu)/(\beta - 1 - q)$.

In both cases, the total infected fraction R_∞ and the maximal extent I_{max} of the disease are reduced; R_∞ satisfying $F(R_\infty, R_0) = 0$ in (4.20), but with $R_0 \mapsto R_0/(1+q)$. It is clear that quarantining will help reduce the impact of the disease.

5.2. Vaccination

Vaccination essentially moves a proportion of the susceptible population to the removed or recovered class. The timing or application of vaccination, however, may differ depending on the circumstances and the accessibility of the vaccines. Here we briefly model three rather ideal scenarios assuming an "all-or-nothing" mechanism for vaccine protection, making references to the two limit cases of $\varepsilon \ll 1$ and both $\varepsilon, \mu \ll 1$. Since those vaccinated are assumed to be all alive they should be distinguished from those in class R (recall a proportion η of which will have died); we will introduce R_v as the vaccinated population fraction.

5.2.1. A pre-infection vaccination programme

Here we consider the case when a fraction r_0 of the population has been vaccinated against the disease by $t = 0$. Assuming the vaccination was not targeted, this has the effect of modifying the initial conditions to $R_v(0) = r_0, S_n(0) = (1-r_0)s_0$ and $S_b(0) = (1-r_0)(1-s_0)$. In both the cases, this will have the effect of reducing the impact of the disease, particularly by reducing the basic reproduction numbers in the $\varepsilon \ll 1$ and $\varepsilon, \mu \ll 1$ cases to $R_0 \sim \beta(1-r_0)s_0$ and $R_0 \sim \beta(1-r_0)$, respectively, thereby increasing the chance of preventing an epidemic.

5.2.2. Vaccination proportional to susceptible population fraction

For this case, the vaccination programme is applied throughout at a rate proportional to the susceptible fraction, this is incorporated into the non-dimensionalised model through equations (2.9) and (2.10),

$$\frac{dS_b}{dt} = -\mu S_b - \beta I_m S_b - \nu S_b, \tag{5.4}$$

$$\frac{dS_n}{dt} = -\beta I_m S_n - \nu S_n, \tag{5.5}$$

$$\frac{dR_v}{dt} = \nu(S_b + S_n), \tag{5.6}$$

where ν is the dimensionless vaccination rate constant; the equations for I_b, I_m and R remain unchanged.

To avoid redoing the analysis of Section 4 to study this problem, we justify the results below using a simple argument. In both the limits analysed, $S_n \sim s_0$ during the lag phase prior to the epidemic; the current modification will lead to $S_n \sim s_0 e^{-\nu t}$. For the vaccination programme to be effective, we need $s_0 - S_n = O(1)$ so that $\nu T_L = O(1)$ or more, hence we may deduce

$\varepsilon \ll 1$ and $\mu = O(1)$. The programme will be totally effective at preventing an epidemic if $(\beta s_0 - 1)/\ln(1/\varepsilon) = 1/T_L \ll \nu$, and will lessen its impact if $\nu = O((\beta s_0 - 1)/\ln(1/\varepsilon)) = O(1/T_L)$.

$\varepsilon \ll 1$ and $\mu \ll 1$. Same again, but the critical quantity for ν is about $(\beta - 1)/\ln(1/\varepsilon\mu) = 1/T_L$.

Since $\varepsilon \ll 1$, the critical level $1/T_L$ is a small quantity, which indicates that the lag phase for the onset of the epidemic buys enough time to allow a "low level" vaccination rate to be effective. Similar investigations based on the standard SIR model would predict that ν needs to be $O(1)$ in order to be effective; this could be a significant over-estimate, which may compromise the application of this vaccination approach in managing the disease. We note that there is no change to R_0 in this analysis.

Figure 7(a) shows the recovered/removed fraction R against time to demonstrate how the vaccination rate ν effects the total proportion of the population that had caught the disease. Here, the relevant case corresponds to $\varepsilon, \mu \ll 1$, and the values used are $\nu = X(\beta - 1)/\ln(1/\varepsilon\mu) = X/T_L$ for $X = 0, 0.1, 0.3, 0.5$ and 0.6. The figure suggests that even at $X = 0.5$ (or $\nu = 1/2T_L$) the vaccination programme significantly reduces the size of the epidemic. The effect of the vaccination rate X on the fraction of the population that catches the disease, R_∞, is shown in Figure 7(b). The analysis predicts that the vaccination programme will be effective when $X = O(1)$, and the numerical results support this. Interestingly, as the infection rate β increases, the removed fraction R_∞ decreases slightly beyond $X \approx 0.6$. The general pattern of the profiles shifting to the right on increasing β ends at about $\beta = 20$, as β increases further (unlikely to be relevant in biological terms) the profiles retreat to the left due to the increased effects of the vaccination rate (as $\nu \propto \beta$ for fixed X) outpacing that of the rate of infection.

5.2.3. Fixed rate vaccination programme

In this case, we consider vaccines that are applied to the susceptible population at a fixed rate ϕ, starting at $t = 0$ when the first case of the bird-human transmissible form is identified.

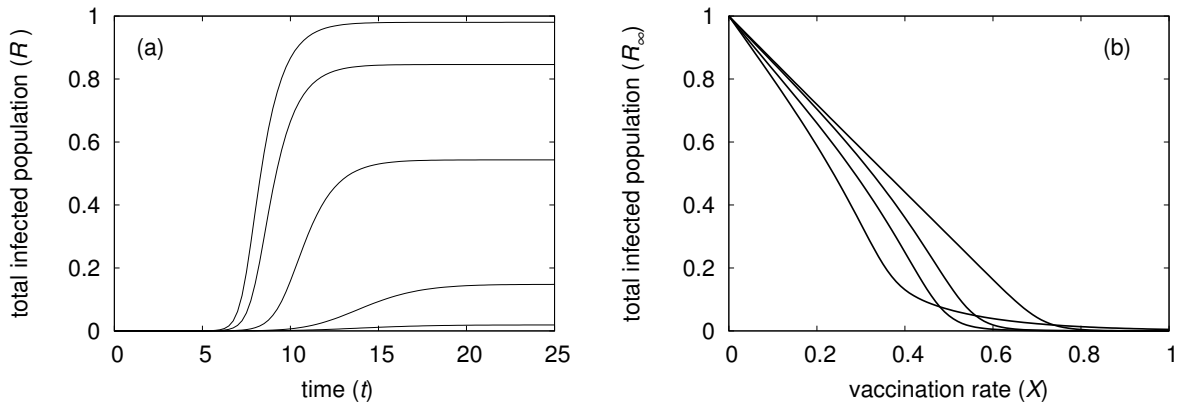

Figure 7: Plot of (a) the recovered/removed fraction R against time and (b) the total fraction that acquire the disease, R_∞, against vaccination rate X (where $\nu = X(\beta-1)/\ln(1/\varepsilon\mu)$). The curves, from left to right, in plot (a) correspond to $X = 0, 0.1, 0.3, 0.5$ and 0.6 and in plot (b) they are $\beta = 2, 3, 4$ and 20. The parameters, unless otherwise stated, are $\beta = 4, \varepsilon = 10^{-4}, \mu = 10^{-4}$ and $s_0 = 0.8$.

This leads to the following modification to the dimensionless equations (2.9), (2.10) and (2.13),

$$\frac{dS_n}{dt} = -\beta I_m S_n - s_0\phi H(S_n), \tag{5.7}$$

$$\frac{dS_b}{dt} = -\mu S_b - \beta I_m S_b - (1-s_0)\phi H(S_b), \tag{5.8}$$

$$\frac{dR_v}{dt} = I_m + I_b + \phi\left(s_0 H(S_n) + (1-s_0)H(S_b)\right), \tag{5.9}$$

where $H(x)$ is the Heaviside step function defined as $H(x) = 0$ for $x \leq 0$ and $H(x) = 1$ otherwise; this is to ensure that the solutions of S_n and S_b remain non-negative.

Using this vaccination programme, the amount of removed susciptibles is proportional to time so will only have an effect if $\phi T_L = O(1)$ or larger. For both the asymptotic limits investigated we can make the same conclusions as those in Section 5.2.2, exchanging ν in the discussion with ϕ.

6. A stochastic model

In the early stages of an epidemic, where only a few individuals have the mutated form of the disease, progression is likely to be very stochastic. For instance, if the rate of catching bird flu and the mutation rate to the transmissible form are both very small, then the population of I_b will be small and individuals with bird flu will most likely be recovered/removed before a mutation event occurs. In such circumstances, a deterministic model may not capture the early stages well and we hence investigate in this section a stochastic form of the model proposed in Section 2. In particular, we will investigate how stochasticity effects features of an epidemic such as the maximum number of individuals infected with the transmissible form, total number of those recovered or removed and the timescales for the onset of the epidemic and its duration.

The proposed stochastic model will take the form of a continuous time Markov process, whereby future states are only dependent on the present one. Using the same variable names as before, the four state variables are $S_n(t), S_b(t), I_b(t)$ and $I_m(t)$, the variable $R(t)$ being derived from (2.6). We will use the term "event" to describe a single transition from one state variable to

Event	Transitional Probability, p_k	$\boldsymbol{I'}$
S_b infected by non-transmittable birdflu	$\mu\, i_1\, \delta t$	(i_1-1, i_2, i_3+1, i_4)
I_b mutated to I_m	$\varepsilon\, i_3\, \delta t$	(i_1, i_2, i_3-1, i_4+1)
S_b infected by mutated flu	$(\beta/N)\, i_1\, i_4\, \delta t$	(i_1-1, i_2, i_3, i_4+1)
S_n infected by mutated flu	$(\beta/N)\, i_2\, i_4\, \delta t$	(i_1, i_2-1, i_3, i_4+1)
I_b infected by mutated flu	$(\beta/N)\, i_3\, i_4\, \delta t$	(i_1, i_2, i_3-1, i_4+1)
I_b recovery/removal	$\gamma\, i_3\, \delta t$	(i_1, i_2, i_3-1, i_4)
I_m recovery/removal	$\gamma\, i_4\, \delta t$	(i_1, i_2, i_3, i_4-1)

Table 2: Transition probabilities from $\boldsymbol{X}(t) = (S_b(t), S_n(t), I_b(t), I_m(t)) = (i_1, i_2, i_3, i_4)$ for each of the seven possible events leading to population $\boldsymbol{X}(t+\delta t) = \boldsymbol{I'}$ as $\delta t \to 0$; each transitional probability has an $o(\delta t)$ error.

another. Let $\boldsymbol{X}(t) = (S_b(t), S_n(t), I_b(t), I_m(t))$ be a state-space vector and let $\boldsymbol{I} = (i_1, i_2, i_3, i_4)$ be a population vector, then Table 2 shows the transition probabilities $p_k = P(\boldsymbol{X}(t+\delta t) = \boldsymbol{I'} \,|\, \boldsymbol{X}(t) = \boldsymbol{I})$, where $k = 1, .., 7$, for each of the seven events as $\delta t \to 0$.

We can, in principle, use these transition probabilities to construct master equations and generating functions to formulate ODEs for the moments [2]. However, as is usual, master equations are difficult to analyse and the formulated ODEs suffers from the identification of suitably reliable moment closure conditions; see [6, 14, 20] and references therein for examples in epidemiological modelling. We will instead analyse the Markov process computationally.

6.1. Comparison between continuum and stochastic model

The stochastic model is simulated using the "the first reaction method" [31]. Here, at each time point a time step, δt_k, is randomly calculated from an exponential distribution with mean p_k for each of the seven events. The event k' that is chosen to occur corresponds to the time step $\delta t_{k'} = \min_{k=1,..,7}\{\delta t_k\}$. We then adjust the population according to event k' and move from $t \mapsto t + \delta t_{k'}$ and repeat the process. The randomly chosen δt_k is computed in the simulations using pseudo-random numbers from an uniform distribution, $U[0,1)$, converted to one satisfying an exponential distribution via inverse transform sampling [31]. In all simulations below, we scale the transition probability parameters so that $\gamma = 1$ and $\beta = 4$, hence the values used for μ and ε are the non-dimensional version of the continuum model.

Figures 8 and 9 compare the mean time profiles from 1000 stochastic simulations with those of the deterministic model. Here, the mean time profile for variable I_m, for example, is defined as

$$\langle I_m \rangle(t) \;=\; \frac{1}{1000} \sum_{p=1}^{1000} I_m^{(p)}(t),$$

where $I_m^{(p)}(t)$ is the population of those infected with the mutant flu at time t in realisation p; the corresponding term for the other variables is similarly defined. In Figure 8, the time profiles of S_n and I_m are shown for $\varepsilon = \mu = 0.01$ (top) and $\varepsilon = \mu = 0.001$ (bottom) for different populations N chosen to demonstrate the varied agreement with the deterministic solutions; here γ, s_0 and β (i.e. R_0 as $\varepsilon = \mu \to 0$) are fixed. As expected, increasing N improves the agreement, whilst increasing the parameters for infection rate from birds μ and the mutation rate ε also improves agreement for fixed N. The latter observation is further demonstrated in Figure 9. The profiles for S_n in Figure 8 (left) show that the point of divergence between

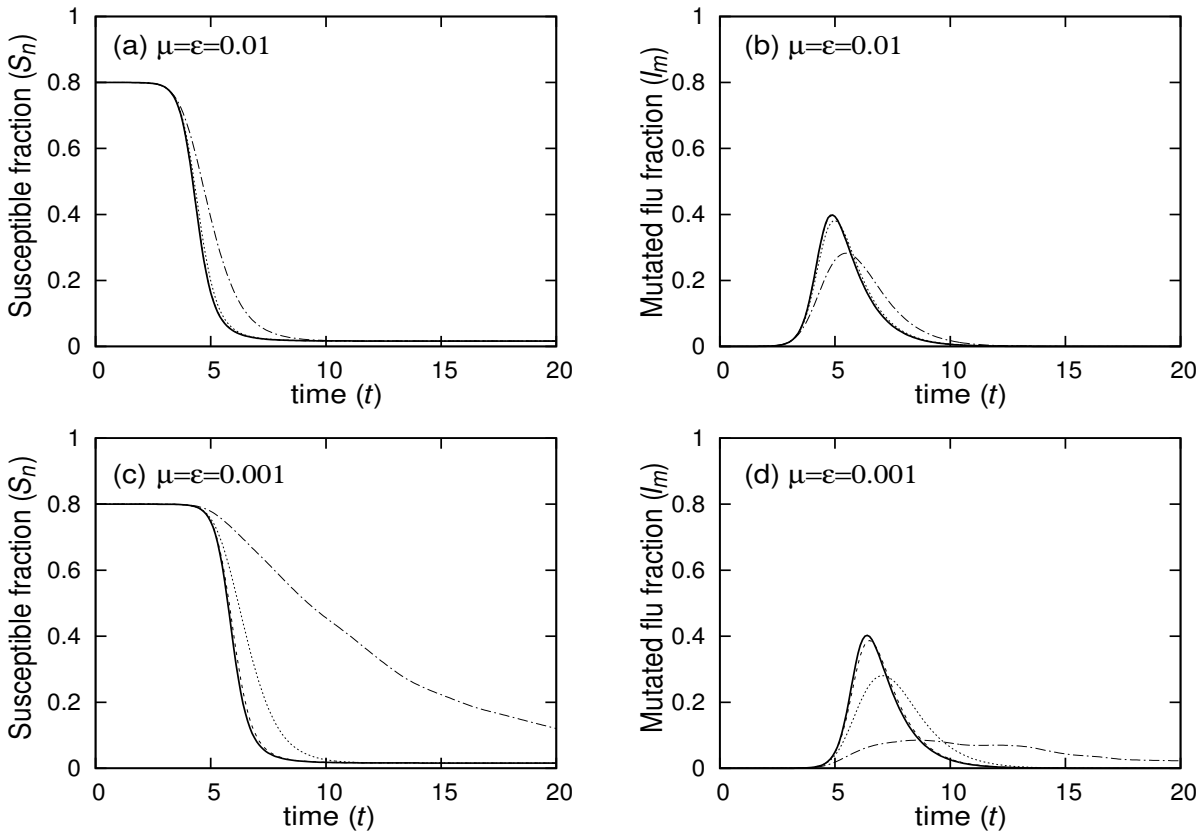

Figure 8: Comparison of the results from deterministic (solid curves) and stochastic (mean of 1000 realisations) simulations. The populations have been normalised to fractions for direct comparison across different total populations N. The left plots compare S_n/N and $\langle S_n\rangle(t)/N$ and the right ones I_m/N and $\langle I_m\rangle(t)/N$, whilst the top and bottom plots are for $\varepsilon = \mu = 10^{-2}$ and $\varepsilon = \mu = 10^{-3}$, respectively. The populations in the top plots are $N = 10^7$ (dashed curves), $N = 10^6$ (dotted curves) and $N = 10^5$ (dash-dotted curves) and for the bottom they are $N = 10^8$ (dashed curves), $N = 10^7$ (dotted curves) and $N = 10^6$ (dash-dotted curves). The other parameters are $\gamma = 1, s_0 = 0.8$ and $\beta = 4$ for all cases.

solutions occurs when the mutated form appears to take hold and infect the entire susceptible class, where for smaller N and/or $\varepsilon = \mu$ the drop in mean density is less steep. Here, the time at which I_m reaches epidemic levels is highly varied (see Figure 10) resulting with a profile for $\langle I_m\rangle(t)$ that is more smeared out.

Figure 10 shows comparisons between the deterministic solutions to four instances of the stochastic simulations, using a parameter set that leads to a highly varied epidemic onset time. On the right of Figure 10 the profiles of the mutated fraction are all very similar, albeit at different time-points at which they reach their peak. Where I_m reaches their peak, the corresponding I_b profile drops down to near zero as shown on the left side of the figure. We note that the deterministic model's prediction of the rising profile of I_b is in good agreement with each of the stochastic runs, where in the latter stochasticity leads to noise about the steady fraction of $I_b \approx \mu(1 - s_0)/\gamma = 2 \times 10^{-5}$. The plots reveal that stochasticity makes little difference with regards to the maximum I_m and duration of infection, this being verified in the results shown in Table 3. Furthermore, the table shows that total number of individuals in the recovered/removed class as $t \to \infty$ are in very good agreement. We note that the standard

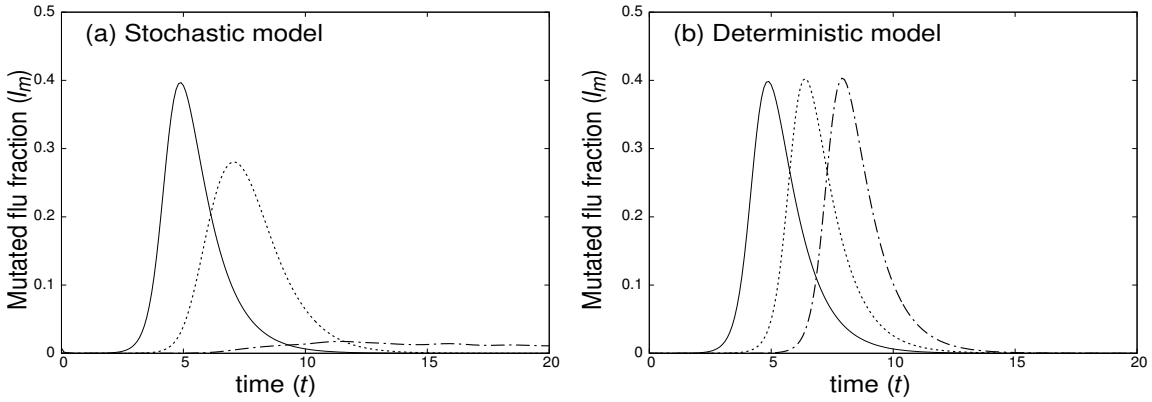

Figure 9: Comparison of stochastic (mean of 1000 realisations, left) and deterministic (right) simulations showing the evolution I_m and $\langle I_m \rangle$ for $\varepsilon = \mu = 10^{-2}$ (solid curves), $\varepsilon = \mu = 10^{-3}$ (dotted curves) and $\varepsilon = \mu = 10^{-4}$ (dashed curves) with $N = 10^7$, $\gamma = 1, s_0 = 0.8$ and $\beta = 4$ in all cases.

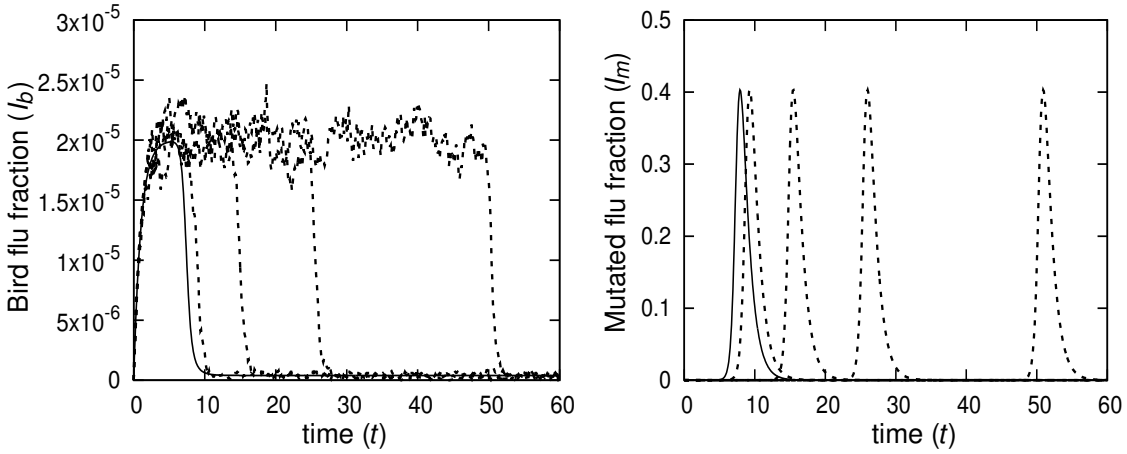

Figure 10: Comparison of the deterministic model solution with 4 realisations of the stochastic model for I_b (left) and I_m (right). Parameters used are $N = 10^7$, $\varepsilon = \mu = 10^{-4}$, $\gamma = 1, s_0 = 0.8$ and $\beta = 4$.

deviations of the stochastic model are less than 1% of the mean in the first three quantities listed. However, where the deterministic model is a poor predictor of stochastic solutions is with regards to the onset of the epidemic, where for smaller values of N, ε and μ it is a severe under-estimate. For this reason, we analyse the stochastic model further to determine analytical estimates for the epidemic onset time in Section 6.2. We investigated the distribution of onset times T_L for a number of values for N, ε and μ; two examples of which are presented in Figure 11, where the probability density functions for T_L is approximated from 10000 realisations in each case. Here, the onset times is split into equal time intervals (or bins) and the frequency of elements from the raw data lying in each bin is normalised so that there is unit area under the curve; the time points in the plot are the mid values in the bins. For larger ε and μ, the shape of the distribution is near bell-shaped, which broadens and skews to the left as ε and μ gets smaller. For the case of $\varepsilon = \mu = 10^{-3}$ (fig. (a)), the profile happens to fit very well to that of the Gumbel distribution (here, the distribution's two parameters are formulated using the mean and standard deviation of the data). However, on comparing all of the probability

	Deterministic	Stochastic
Maximum I_m	4.0333×10^6	$4.0237 \times 10^6 \pm 1.0146 \times 10^4$
Duration of epidemic, $I_m > \sigma N$	9.8698	9.8742 ± 0.084654
Total infected, R_∞	9.8413×10^6	$9.8404 \times 10^6 \pm 1.0129 \times 10^3$
Epidemic lag time T_L	5.2031	70.548 ± 66.949

Table 3: Table showing comparisons between the deterministic solutions and the means of 10000 realisations of the stochastic model, with one standard deviation shown. Here, T_L is defined so that $I_m(T_L) = 10^{-3}N$ where $N = 10^7$; other parameters are $\varepsilon = \mu = 10^{-4}$, $\gamma = 1, s_0 = 0.8$ and $\beta = 4$. All realisations had an epidemic phase.

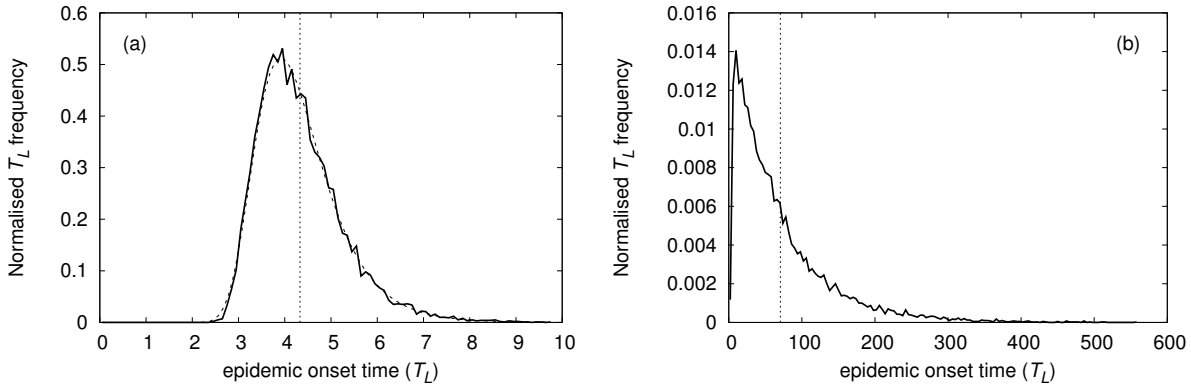

Figure 11: Approximations of the probability density function for epidemic onset time, T_L, generated from 10000 realisations of the stochastic model. Plot (a) shows the case of $\varepsilon = \mu = 10^{-3}$ (solid, bin width of 0.1) together with Gumbel distribution (dashed) formulated from the mean and standard deviation of the realisations. Plot (b) shows the case of $\varepsilon = \mu = 10^{-4}$, plotted with a bin width of 4. The vertical dotted line indicates the mean. The remaining parameters are $N = 10^7$, $\gamma = 1, s_0 = 0.8$ and $\beta = 4$.

distributions available in the mathematics package MATLAB with all of the results generated from the stochastic simulations, no single distribution fits the data well in all cases (indeed all these distributions poorly fitted that shown in the right plot); hence this was not pursued further. Figure 11(b) shows the case $\varepsilon = \mu = 10^{-4}$, where, interestingly, the modal value of $T_L \approx 10$ in the plot is much closer to that predicted by the deterministic model.

6.2. Expected time for the epidemic onset

Described in Appendix C are two formulations to estimate the expected time of the epidemic onset T_L. Both formulations assume that during the progression of the epidemic when $t < T_L$, the infected populations are negligible in comparison to the uninfected classes, hence $S_b + S_n = N$ is assumed. The first formulation, described in Appendix C.1, assumes that the rise in I_b and I_m occur independently and the estimate of $E(T_L)$ is made by summing the time for I_b to reach a pseudo-steady state $I_b = I_b^c = \mu(1 - s_0)N/\gamma$, giving say $E(T_1)$ and the time for I_m to reach σN given $I_b = I_b^c$, say $E(T_2)$; hence $E(T_L) \approx E(T_1) + E(T_2)$. This can be calculated easily, but is a flawed estimate since the rising of I_b and I_m are not independent. The second formulation considers changes in both I_b and I_m leading to a two-variable recurrence relation to obtain $E(T_L)$. This formulation, if solved directly, is very computationally intensive, particularly for large N and less small ε and μ; described in Section C.2 is a method to obtain a good estimate of the solution more efficiently.

The bullets in Figure 12 show the mean epidemic onset time from 1000 trials of stochastic

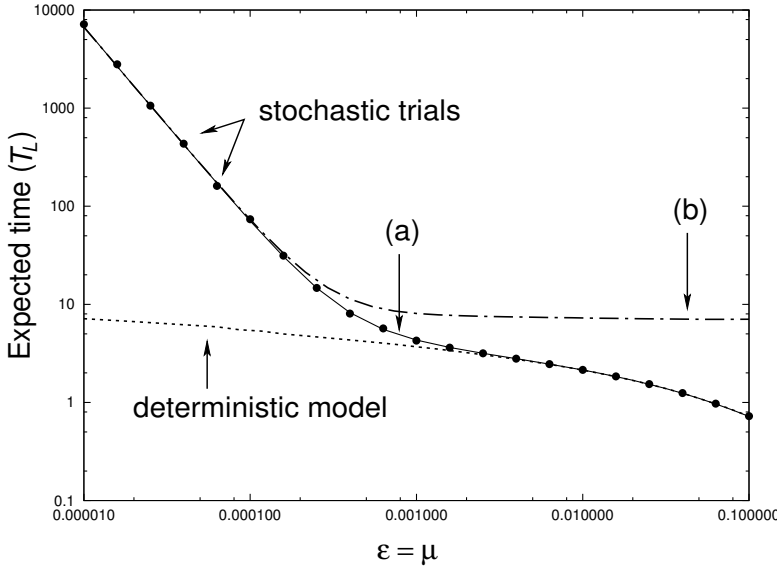

Figure 12: Comparison of estimates for the onset of an epidemic defined to be when $I_m = \sigma N$ with $\sigma = 10^{-3}$ and $N = 10^7$, as a function of $\varepsilon = \mu$. The plots shows the mean onset time from 1000 trials of the stochastic model (bullets), that predicted by the deterministic model (dotted line), and the two estimates of $E(T_L)$ described in Appendix C, namely $E(T_1) + E(T_2)$ from Appendix C.1 (dot-dashed line, curve (b)) and $E(0,0)$ described in Appendix C.2 (solid line, curve (a)). The other parameters are $\gamma = 1, s_0 = 0.8$, $\beta = 4$ and $\rho = 1.5$ (see Appendix C).

model simulations at points between $\varepsilon = \mu = 10^{-5}$ to $\varepsilon = \mu = 10^{-1}$ for $N = 10^7$. This shows the rapid increase in $E(T_L)$ as parameters $\varepsilon = \mu$ decrease. The dotted line shows that the deterministic model is a very poor approximation for small $\varepsilon = \mu$, but become very good beyond $\varepsilon = \mu \approx 10^{-3}$. Conversely, the first formulation, curve (b), estimates $E(T_L)$ well for very small $\varepsilon = \mu$, but fails to be a good prediction beyond $\varepsilon = \mu \approx 3.10^{-4}$; this suggests that assuming independence of I_b and I_m is reasonable when $\varepsilon = \mu$ are very small. However, the estimate from the second formulation, curve (a), is in very good agreement across the entire range, suggesting that the constant uninfected population assumption is reasonable. We note, that by increasing N improves the deterministic model's prediction of $E(T_L)$, as expected; for example, using $\mu = \varepsilon = 10^{-4}$ and (currently unrealistic) $N = 10^{10}$, the stochastic simulation mean from a 1000 trials gives $E(T_L) \approx 5.24$ is close to the deterministic model's estimate of $T_L \approx 5.20$.

7. Conclusion

In this paper, a simple mathematical model is constructed to study the outbreak of an infectious disease following mutation of a non-transmissible strain for which only a subset of the population are at risk of catching. This scenario may arise in avian flu, in which currently only people working with poultry are likely to catch the disease, but a mutation could lead to a human-human spreading strain, with potentially devastating results. We derived a mathematical model extending an SIR type approach that divides each of the susceptible and infectious classes into two subclasses. The susceptibles were divided into those who are (e.g. poultry farmers) or are not at risk of catching bird-human strain and those who are infected with the bird-human and human-human transmissible strains. We note, the assumed division of susceptibles into two

(or more) classes has very wide application, where sub-populations with distinct disease exposure characteristics to the non-mutated form could be based on activity, geography or demography. The model has relatively few parameters and four dimensionless ones (β, μ, ϵ and s_0), of these s_0 could be obtainable using suitable census data and using ordinary flu for the infection rates we may expect β to be in the range $2-5$ [8, 22]. Estimation of μ and ϵ will be more difficult and will require clinical data and perhaps laboratory data for estimates of mutation rates.

Analysis of the model was aimed at predicting the severity of an epidemic in terms of the model's parameter values. In particular, we sought to establish the necessary conditions for an epidemic to occur and key characteristics such as the timescale for the onset of the epidemic, the size and duration of the epidemic and the maximum level of the infected individuals at one time. For general parameter values, we derived in Section 3 bounds on the predicted total fraction of the population who will catch the disease. Further progress was made in two biologically feasible asymptotic limits in Section 4 using singular perturbation theory. Here, analytical approximations to the model solutions were made by solving systematically deduced reduced systems for different timescales, making it easier to identify the important processes at various stages of the epidemic and to express key epidemic features in terms of simple formulae (as summarised in Table 1). In particular, it was demonstrated that the naive assertion of the reproduction number $R_0 = \beta$ (dimensionless) would not be appropriate for small ε and $\mu \sim 1/\ln(1/\varepsilon)$ or larger (equation (4.21)). Furthermore, the analysis highlighted the role of parameters ε and μ on the logarithmic dependence on the timescale for epidemic onset, T_L, whilst other aspects of an epidemic (duration, maximum infectives etc.) are largely governed by an SIR model and parameters β and s_0. However, it is in the prediction of T_L, for very small ε and μ and insufficiently large populations, where the deterministic model fails, as demonstrated in Section 6 using a stochastic model; the rarity of mutation events combined with failure to pass on the infection result in extended onset times. This highlights the need for caution when using a deterministic model to describe the progress of a disease in "large populations", as the presence of small parameters may necessitate the population to be much larger than expected (perhaps beyond that which is applicable) for the model to represent well the mean of a stochastic process. However, in all other key features of an epidemic, the results of the deterministic and stochastic models were in very good agreement.

In Section 5, the model is extended to investigate the effect of a range of quarantine and vaccination programmes. The simple formulations resulting from asymptotic analysis made it a relatively simple task to predict the outcome of such measures and, in particular, indicate how intensively the measures need to be applied in order for them to be effective. They target two characteristics of the disease predicted by the model: 1) by reducing the effective basic reproduction number (specifically in the cases of quarantine and pre-infection vaccination programmes) and 2) by exploiting the time lag prior to the epidemic, whereby a significant proportion of the population will be vaccinated before the outbreak. Of course, the situation is more complicated than that assumed in the model, with the existence of many and newly evolving flu virus strains and the constant need to develop new vaccines. Without suitable estimates of all the parameters, it is difficult to assert which programme will be the most effective. However, the analysis confirms what is surely well known, that all measures will help and should be implemented.

The infection-mutation pathway assumed in the formulation of the models is intentionally simple for analytical tractability, enabling a number of insights to be drawn in the possible dynamics of epidemics resulting from a mutation; though, for example, the asymptotic analysis of Section 4 can in principle be applied to much larger systems. Of course, such modelling simplifications are made at a cost of a number of potentially important details. The model can

be refined to consider other phases (e.g. incubation phase), population classes (e.g. bird populations), endemic scenario (population growth and migration), time dependent infectiousness and recovery (e.g. integro- and/or delay- differential equation systems), and spatial effects (either as a continuum or in a patch network). These refinements will doubtless lead to a models with better predictive capabilities in more specific scenarios. Nevertheless, the current model serves as a simple approximation to describe the emergence of mutated, spreadable disease, that is simple enough to analyse in some detail and so provide insight into the timing and appropriate use of control measures should the threat of an epidemic becomes imminent; for avian flu, we hope this will never be the case.

Acknowledgements

CYC and JW would like to thank the Ministry of Science and Technology of Taiwan (MOST) for funding an academic visit to Taiwan. CYC would also like to thank MOST for the funding of the project (105-2115-M-390-003).

References

[1] Alexander DJ. A review of avian influenza in different bird species. *Vet. Microbiol.* (2000) **74**, 3-13.

[2] Allen LJS. An Introduction to Stochastic Processes with Applications to Biology. Chapman and Hall/CRC Press; 2nd edition (2010).

[3] Andreasen, V. The Final Size of an Epidemic and Its Relation to the Basic Reproduction Number. *Bull. Math. Biol.* (2011) **73**, 2305-2321.

[4] Boender GJ, Hagenaars TJ, Bouma A, Nodelijk G, Elbers ARW, de Jong MCM and van Boven M. Risk Maps for the Spread of Highly Pathogenic Avian Influenza in Poultry. *PLoS Comp. Biol.* (2007) **3**, 704-712.

[5] Boni MF, Gog JR, Andreasen V and Feldman MW. Epidemic dynamics and antigenic evolution in a single season of influenza A. *Proc. R. Soc. B* (2006) **273**, 1307-1316.

[6] Chalub FACC and Souza MO. The SIR epidemic model from a PDE point of view. *Math. Comp. Mod.* (2011) **53**, 1568-1574.

[7] Chong NS, Tchuenche JM and Smith RJ. A mathematical model of avian influenza with half-saturated incidence. *Theory Biosci.* (2014) **133**, 23-38.

[8] Chowell G, Nishiura H and Luís MA. Comparative estimation of the reproduction number for pandemic influenza from daily case notification data. *J. R. Soc. Interface* (2006) **4**, 155-166.

[9] Cooke KL. Stability analysis for a vector disease model. *Rocky Mountain Journal of Mathematics* (1979) **7**, 253-263.

[10] Ferguson NM, Galvani AP and Bush RM. Ecological and immunological determinants of influenza evolution. *Nature* (2003) **422**, 428-433.

[11] Girvan M, Gallaway DS, Newman MEJ and Strogatz SH. Simple model of epidemics with pathogen mutation. *Phys. Rev E* (2002) **65**, 031915.

[12] Greger M. The human/animal interface: Emergence and resurgence of zoonotic infectious diseases. *Critical Review in Microbiology* (2007) **33**, 243-299.

[13] Gumel AB, Global dynamics of a two-strain avian influenza model. *Int. J. Comp. Math.* (2009), **86**,85-108.

[14] Isham V. Assessing the variability of stochastic epidemics. *Math. Biosci.* (1991), **107**, 209-224.

[15] Iwami S, Takeuchi Y and Liu X. Avian-human influenza epidemic model. *Math. Biosci.* (2007) **207**, 1-25.

[16] Jin Z and Ma Z. The stability of an SIR epidemic model with time delays. *Math. Biosci. Eng.* (2006) **3**, 101-109.

[17] Källén A, Arcuri P and Murray JD. A simple model for the spatial spread and control of rabies. *J. Theor. Biol.* (1985) **116**, 377-393.

[18] Kermack WO and McKendrick AG. A Contribution to the Mathematical Theory of Epidemics. *Proc. Roy. Soc. A* (1927) **115**, 700-721.

[19] Korobeinikov A and Maini PK. A Lyapunov function and global properties for SIR and SEIR epidemiological models with nonlinear incidence. *Math. Biosci. Eng.* (2004) **1**, 57-60.

[20] Krishnarajah I, Cook A, Marion G and Gibson G. Novel moment closure approximations in stochastic epidemics. *Bull. Math. Biol.* (2005) **67**, 855-873.

[21] Le Menach A, Vergu E, Grais RF, Smith DL and Flahault A. Key strategies for reducing spread of avian influenza among commercial poultry holdings: lessons for transmission to humans. *Proc. R. Soc. B* (2006) **273**, 2467-2475.

[22] Lin J, Andreasen V, Casagrandi R and Levin SA. Traveling waves in a model of influenza A drift. *J. Theor. Biol.* (2003) **222**, 437-445.

[23] Martcheva M. Avian flu: modeling and implications for control. *J. Biol. Syst.* (2014) **22**, 151-175.

[24] Miller JC. A note on the derivation of epidemic final sizes. *Bull. Math. Biol.* (2012) **74(9)**, 2125-2141.

[25] Murray JD, 1993. Mathematical Biology, 2nd edition. Springer-Verlag, Berlin.

[26] Pease CM. An evolutionary epidemiological mechanism with applications to Type A Influenza. *Theor. Pop. Biol.* (1987) **31**, 422-452.

[27] Sharke KJ, Bowers RG, Morgan KL, Robinson SE and Christley RM. Epidemiological consequences of an incursion of highly pathogenic H5N1 avian influenza into the British poultry flock. *Proc. R. Soc. B*, (2008) **275**, 19-28.

[28] Scholtissek C. Source for influenza pandemics. *Eur. J. Epidemiol.*, (1994)**10**, 455-458.

[29] Tapper ML. Emerging viral diseases and infectious disease risks. *Haemophilia* (2006) **12**, 3-7.

[30] Tchuenche JM, Nwagwo A and Levins R. Global behaviour of an SIR epidemic model with time delay. *Math. Meth. Appl. Sci.* (2007) **30**, 733749.

[31] Toral R and Colet P, 2014. Stochastic Numerical Methods, Wiley-VCH; 1st edition (2014).

[32] Tornatore E, Buccellato SM and Vetro P. Stability of a stochastic SIR system. *Physics A* (2005) **354**, 111-126.

[33] Tuckwell HC and Williams RJ. Some properties of a simple stochastic epidemic model of SIR type. *Math. Biosci.* (2007) **208**, 76-97.

[34] Wang R-H, Jin Z, Liu Q-X, van de Koppel J, Alonso D (2012) A Simple Stochastic Model with Environmental Transmission Explains Multi-Year Periodicity in Outbreaks of Avian Flu. PLoS ONE 7(2): e28873. doi:10.1371/journal.pone.0028873.

[35] Wonham MJ, de-Camino-Beck T and Lewis MA. An epidemiological model for West Nile virus: invasion analysis and control applications. *Proc. R. Soc. B* (2004) **271**, 501-507.

[36] World Health Organization (WHO), Ebola Virus Disease Outbreak, Situation Reports, December 2015. Website: `http://www.who.int/ebola/en/`.

[37] World Health Organization (WHO), programmes and project report. Cumulative number of confirmed human cases of avian influenza A/(H5N1) reported to WHO, December 14th 2015. Website: `http://www.who.int/influenza/human_animal_interface/H5N1_cumulative_table_archives/en/`

Appendix A. Derivation of equation (4.21) for R_0 as $\varepsilon \to 0$

In this appendix we determine an approximation to the surface $R_0 = 1$, as defined by Definition 2.1, in parameter space as $\varepsilon \to 0$. The analysis of Section 4.1 (where $\varepsilon, \mu \to 0$) demonstrated that $R_0 = \beta$ and in Section 4.2 ($\varepsilon \to 0, \mu = O(1)$) it was stated that $R_0 = \beta s_0$. As described in Section 4 the transition between the values of R_0 occurs in the distinguished limit $\mu \sim 1/\ln(1/\varepsilon)$ as $\varepsilon \to 0$. Writing

$$\mu \;=\; \frac{\overline{\mu}}{L}, \qquad L \;=\; \ln(1/\varepsilon),$$

and take as the initial scalings for $t = O(1)$,

$$t \;=\; t^{\diamond}, \quad S_b \;=\; S_b^{\diamond}, \quad S_n \;=\; S_n^{\diamond}, \quad I_b \;=\; \frac{I_b^{\diamond}}{L}, \quad I_m \;=\; \frac{\varepsilon}{L}\, I_m^{\diamond},$$

leads to the system

$$\frac{dS_b^{\diamond}}{dt^{\diamond}} \;=\; -\frac{\overline{\mu}}{L} S_b^{\diamond} \;-\; \frac{\varepsilon}{L}\, \beta\, I_m^{\diamond} S_b^{\diamond}, \tag{A.1}$$

$$\frac{dS_n^{\diamond}}{dt^{\diamond}} \;=\; -\frac{\varepsilon}{L}\, \beta\, I_m^{\diamond} S_n^{\diamond}, \tag{A.2}$$

$$\frac{dI_b^{\diamond}}{dt^{\diamond}} \;=\; \overline{\mu}\, S_b^{\diamond} \;-\; I_b^{\diamond} \;-\; \varepsilon\, I_b^{\diamond} \;-\; \frac{\varepsilon}{L}\, \beta\, I_m^{\diamond} I_b^{\diamond}, \tag{A.3}$$

$$\frac{dI_m^{\diamond}}{dt^{\diamond}} \;=\; I_b^{\diamond} \;+\; \beta\, I_m^{\diamond}\, (S_b^{\diamond} + S_n^{\diamond}) \;-\; I_m^{\diamond} \;+\; \frac{\beta}{L}\, I_m^{\diamond}\, I_b^{\diamond}, \tag{A.4}$$

subject to $S_b^\diamond(0) = 1-s_0, S_n^\diamond(0) = s_0, I_b^\diamond(0) = 0$ and $I_m^\diamond(0) = 0$. A full analysis involves making expansions of the form $S_b^\diamond \sim S_b^{\diamond[0]} + \varepsilon S_b^{\diamond[1]}$, whereby each of $S_b^{\diamond[i]}$ are expressed in powers of L^{-1} (likewise for the other variables). For a leading order estimate of R_0 we only need the terms with subscript [0]. Solving the leading terms in (A.1)-(A.3) we obtain

$$S_b^{\diamond[0]} \;=\; (1-s_0)\sum_{n=0}^{\infty}\frac{(-1)^n(\overline{\mu}\,t^\diamond)^n}{n!\,L^n} \;=\; (1-s_0)\,e^{-\overline{\mu}\,t^\diamond/L}, \qquad S_n^{\diamond[0]} \;=\; s_0,$$

$$I_b^{\diamond[0]} \;=\; \overline{\mu}(1-s_0)\,\frac{\left(e^{-\overline{\mu}\,t^\diamond/L}-e^{-t^\diamond}\right)}{1-\overline{\mu}/L},$$

where shown for $S_b^{\diamond[0]}$ is the derived infinite series in powers of $1/L$ conveniently collapsing to an exponential form. Equation (A.4) becomes

$$\frac{dI_m^{\diamond[0]}}{dt^\diamond} \;=\; I_b^{\diamond[0]} \;+\; f(t^\diamond)\,I_m^{\diamond[0]}, \tag{A.5}$$

where $f(t) = \beta\left(s_0 + (1-s_0)e^{-\overline{\mu}\,t/L}\right) - 1$. This solves to give

$$I_m^{\diamond[0]} \;\sim\; A_0(t^\diamond)\,\exp\left((\beta s_0 - 1)\,t^\diamond + \beta(1-s_0)\,\frac{(1-e^{-\overline{\mu}t^\diamond/L})}{\overline{\mu}/L}\right), \tag{A.6}$$

where $A_0(t^\diamond) \geq 0$ is given by

$$A_0(t^\diamond) = \overline{\mu}(1-s_0)\int_0^{t^\diamond}\exp\left(F(z)\right)\frac{(e^{-\overline{\mu}z/L}-e^{-z})}{1-\overline{\mu}/L}\,dz, \tag{A.7}$$

with $F(z) = -(\beta s_0 - 1)\,z - \beta(1-s_0)L(1-e^{-\overline{\mu}z/L})/\overline{\mu}$, noting that $F'(z) = -f(z)$. In the case of $R_0 > 1$, it is required that $I_m^{\diamond[0]}$ rises to $O(1/\epsilon)$ in order for the disease to progress to an epidemic. As in Section 4.1.1 this will occur in a timescale $t^\diamond \sim \ln(1/\epsilon)/T$, for some value T. In our estimate for the parameter formulation corresponding to $R_0 = 1$, we define T^* so that at $t^\diamond = \ln(1/\epsilon)/T^*$ we have

$$\text{(i)}\;\; I_m^{\diamond[0]}(L/T^*) \;=\; \frac{1}{\epsilon}, \qquad \text{(ii)}\;\; \frac{dI_m^{\diamond[0]}}{dt^\diamond}(L/T^*) \;=\; 0; \tag{A.8}$$

the second condition implies that $I_m^{\diamond[0]}(L/T) = 1/\epsilon$ is the maximum extent of population fraction with the transmissible form. If $I_m^{\diamond[0]} \sim 1/\epsilon$ then condition (ii) reduces to

$$f(L/T^*) \;=\; \beta\left(s_0 + (1-s_0)\,e^{-\overline{\mu}/T^*}\right) \;-\; 1 \;=\; 0, \tag{A.9}$$

at leading order. We note for $t^\diamond \in [0, L/T^*)$, it is straightforward to show that $f'(t^\diamond) < 0$ and hence $f(t^\diamond) > 0$. We can deduce immediately from (A.9) that

$$1 \;\leq\; \beta \;\leq\; \frac{1}{s_0}, \tag{A.10}$$

at $t^\diamond = \ln(1/\epsilon)/T^*$ on $R_0 = 1$.

Writing down condition (i) in algebraic form is made difficult by being unable to integrate (A.7) in terms of commonly used functions, however, we can derive upper and lower bounds for

$A_0(L/T^*)$ in the limit $\epsilon \to 0$ (or $L \to \infty$) that are both of size $O(1)$. To do this, it useful to note that since $F(0) = 0$ and that $F'(z) = -f(z) \leq 0$ and $F''(z) > 0$ in the domain $t^\diamond \in [0, L/T^*]$, then $F(z) < 0$ and is convex in this domain. Noting further that $(1 - e^{-ax})/a < x$ for $a, x > 0$, then $F(z)$ can be bounded as follows

$$-(\beta s_0 - 1)\, z - \beta(1 - s_0)z = -(\beta - 1)\, z \;<\; F(z) \;<\; F(L/T^*)\frac{T^*}{L}\, z \;<\; 0,$$

the second inequality resulting from convexity of $F(z)$. Writing $X = -F(L/T^*)T^*$, so that $X > 0$, then by substituting these upper and lower bounds on $F(z)$ into (A.7) and integrate yields the following bounds on $A_0(L/T^*)$,

$$\frac{\overline{\mu}(1 - s_0)}{\beta\,(\beta - 1)} \;<\; A_0(L/T^*) \;<\; \frac{\overline{\mu}(1 - s_0)}{X\,(X + 1)}, \tag{A.11}$$

as $L \to \infty$. In the limit of $\varepsilon \to 0$, the bounds are positive, $O(1)$ in size and independent of ϵ. For case (i) in (A.8), taking the logarithm of (A.6), dividing through by $\ln(1/\epsilon)$ and using from (A.11) that $\ln(A_0)/L \ll 1$, the second condition on $R_0 = 1$ is therefore given by,

$$\frac{(\beta s_0 - 1)}{T^*} \;+\; \frac{\beta(1 - s_0)}{\overline{\mu}}\,(1 - e^{-\overline{\mu}/T^*}) \;=\; 1, \tag{A.12}$$

at leading order as $L \to \infty$. Solving for T^* in (A.9) gives $T^* = \overline{\mu}/\ln(\beta(1 - s_0)/(1 - \beta s_0))$, so that equation (A.12) leads to the following equation on $R_0 = 1$,

$$\overline{\mu} \;=\; \beta - 1 \;-\; (1 - \beta s_0)\ln\left(\frac{\beta(1 - s_0)}{1 - \beta s_0}\right), \tag{A.13}$$

as $\varepsilon \to 0$. Equation (A.13) is real for $\beta < 1/s_0$, and from the limit of $\beta \to 1/s_0^-$ we deduce that the formula is only valid for $\overline{\mu} < (1 - s_0)/s_0$. If $\overline{\mu} \geq (1 - s_0)/s_0$ then $\beta = 1/s_0$ along $R_0 = 1$, as $dI_m^{\diamond[0]}/t^\diamond > 0$ in equation (A.5) is guaranteed if $\beta > 1/s_0$ as $t^\diamond \to \infty$. A useable definition of R_0 is thus

$$R_0 \;=\; \begin{cases} \beta \;-\; (1 - \beta s_0)\ln\left(\dfrac{\beta(1 - s_0)}{1 - \beta s_0}\right) \;-\; \overline{\mu} & \overline{\mu} \;<\; (1 - s_0)/s_0, \\ \beta s_0 & \overline{\mu} \;\geq\; (1 - s_0)/s_0, \end{cases} \tag{A.14}$$

in the limit $\varepsilon \to 0$. Writing $\overline{\mu} = \mu \ln(1/\varepsilon)$ leads to the form shown in equation (4.21).

We note that if $R_0 > 1$, then the analysis above only describes conditions for $I_m = O(1/\ln(1/\varepsilon))$, rather than $I_m = O(1)$ as stipulated in Definition 2.1. In the subsequent timescale, $S_b \sim$ constant as I_m continues to grow exponentially, leading to breakdown when the new $I_m = O(\ln(1/\varepsilon))$, occurring on an additional $\ln(\ln(1/\varepsilon))$ timescale to that above. Consequently, there will an error of size $O(\ln(\ln(1/\varepsilon)))/\ln(1/\varepsilon) \ll 1$ to the formula in R_0. As this error is small, (A.14) is applicable as a leading order estimate for the full definition of R_0 in this paper. The remaining analysis for this case is similar to that described in Sections 4.1.2 and 4.1.3 and is not discussed further.

Appendix B. Duration of the epidemic in the limit $\beta \to \infty$

In this appendix we aim to determine approximately the duration T_σ of the epidemic, which is defined here to be the period of time at which $I_m \geq \sigma$, where constant $\sigma \in (0, 1)$ is a suitably

significant fraction of the population. We will seek solutions in the large infectious rate limit, $\beta \to \infty$, in order to obtain solutions to the variables as explicit functions of time and hence the disease duration can be approximated. We are assuming that $\epsilon\,\beta \ll 1$ so that the analysis below is a special case to that of Section 4.1.3. We will recast the problem of that section to an equivalent initial value problem, namely

$$\frac{dS_0}{dt} = -\beta I_m S_0, \tag{B.1}$$

$$\frac{dI_m}{dt} = \beta I_m S_0 - I_m, \tag{B.2}$$

subject to

$$t = 0: \qquad S_0 = s_0 - \sigma,\ I_m = \sigma; \tag{B.3}$$

for the problem in Section 4.1.3 we have $s_0 = 1$, but we will keep it as s_0 in the analysis below, as it is of relevance for the $\mu = O(1)$ case discussed in Section 4.2 provided that $\beta \ll \ln(1/\varepsilon)$. In the latter case, having $1 \ll T_L \sim \ln(1/\varepsilon)/(\beta s_0 - 1)$ ensures that $S_b, I_b \sim 0$ before $I_m \sim \sigma$, so the susceptible pool is only those in population S_n; if $\beta \sim \ln(1/\varepsilon)$ or larger then setting $s_0 = 1$ gives a good approximation. The system (B.1)-(B.3) is the classic SIR model and it does seem likely that the analysis below has been reported before in some form; however, we have not found any such reference and hence its inclusion here. We note the problem to determine the epidemic duration is a shooting problem, in which we impose the boundary condition $I_m(T_\sigma) = \sigma$ to determine T_σ; this could be routinely solved numerically. However, for there to be a solution $T_\sigma > 0$, dI_m/dt must be positive at $t = 0$, hence $\beta > 1/(s_0 - \sigma)$; this is the condition on β for the epidemic to reach the level $I_m = \sigma$.

In the limit $\beta \to \infty$ there are three timescales of interest, namely $t = O(1/\beta)$, $t = \ln(\beta)/\beta s_0 + O(1/\beta)$ and $t = O(1)$, the latter timescale leading to the approximate value of T_σ.

B.1. $\boldsymbol{t = O(1/\beta)}$

Since β is large, the disease is highly infectious and will rapidly spread through the entire susceptible population, hence there is this very small initial timescale. Writing

$$t = \frac{\tilde{\tau}}{\beta}, \quad S_n = \tilde{S}_n, \quad I_m = \tilde{I}_m,$$

leads to

$$\frac{d\tilde{S}_n}{d\tilde{\tau}} = -\tilde{I}_m \tilde{S}_n, \tag{B.4}$$

$$\frac{d\tilde{I}_m}{d\tilde{\tau}} = \tilde{I}_m \tilde{S}_n - \frac{1}{\beta}\tilde{I}_m, \tag{B.5}$$

which has the leading order solutions

$$\tilde{S}_n \sim \frac{s_0(s_0 - \sigma)}{s_0 - \sigma + \sigma e^{s_0\tilde{\tau}}}, \qquad \tilde{I}_m \sim \frac{\sigma s_0 e^{s_0\tilde{\tau}}}{s_0 - \sigma + \sigma e^{s_0\tilde{\tau}}}. \tag{B.6}$$

Correction terms for $\tilde{S}_n$ and $\tilde{I}_m$ can be found but involve somewhat unwieldy special functions, however, for matching in the next timescale, we only need the expansion of the sum of $\tilde{S}_n$ and $\tilde{I}_m$, namely

$$\tilde{S}_n + \tilde{I}_m \sim s_0 + \frac{1}{\beta}\left(\ln(s_0) - s_0\tilde{\tau} - \ln(\sigma + (s_0 - \sigma)e^{-s_0\tilde{\tau}}\right). \tag{B.7}$$

As $\tilde{\tau} \to \infty$, we can show up to β^{-1} that $\tilde{S}_n + \tilde{I}_m \sim \tilde{I}_m$, hence

$$\tilde{S}_n \sim \frac{s_0(s_0-\sigma)}{\sigma} e^{-s_0\tilde{\tau}}, \qquad \tilde{I}_m \sim s_0 + \frac{1}{\beta}\left(\ln\left(\frac{s_0}{\sigma}\right) - s_0\tilde{\tau}\right), \tag{B.8}$$

from which it is confirmed that, to leading order, the entire population will become infected with the disease. These expansions will remain valid until $\tilde{S}_n \sim 1/\beta$, i.e. $\tilde{\tau} \sim \ln(\beta)/s_0$, when there will be a change of balance in equation (B.5).

B.2. $\boldsymbol{t = \ln(\beta)/\beta s_0 + O(1/\beta)}$

Here the disease has reached its peak. We write

$$t = \frac{\ln(\beta)}{\beta s_0} + \frac{\tilde{\tau}^*}{\beta}, \quad S_n = \frac{1}{\beta}\tilde{S}_n^*, \quad I_m = \tilde{I}_m^*,$$

to get

$$\frac{d\tilde{S}_n^*}{d\tilde{\tau}^*} = -\tilde{I}_m^*\tilde{S}_n^*, \tag{B.9}$$

$$\frac{d\tilde{I}_m^*}{d\tilde{\tau}^*} = \frac{1}{\beta}\left(\tilde{I}_m^*\tilde{S}_n^* - \tilde{I}_m^*\right), \tag{B.10}$$

which leads to

$$\begin{aligned} \tilde{S}_n^* &\sim \frac{s_0(s_0-\sigma)}{\sigma} e^{-s_0\tilde{\tau}^*}, \\ \tilde{I}_m^* &\sim s_0 - \frac{1}{\beta}\left(\ln(\beta) + s_0\tilde{\tau}^* - \ln\left(\frac{s_0}{\sigma}\right) + \frac{s_0(s_0-\sigma)}{\sigma} e^{-s_0\tilde{\tau}^*}\right), \end{aligned} \tag{B.11}$$

where we have matched with expansions (B.8) as $\tilde{\tau}^* \to -\infty$ and $\beta \to \infty$. Here the number of susceptibles decays to exponentially small levels, whilst the infected fraction remains relatively unchanged. As $\tilde{\tau}^* \to \infty$, the expansion breaks down when $\tilde{\tau}^* \sim \beta$ as recovery/removal of the infected individuals becomes apparent.

B.3. $\boldsymbol{t = O(1)}$

After the very rapid spread of the disease over the entire remaining susceptible population, the epidemic declines over an $O(1)$ timescale. The fraction of susceptibles is exponentially small and can now be neglected and so our only concern is with the infected fraction. Writing

$$t = \bar{\tau}, \quad I_m = \bar{I}_m,$$

gives

$$\frac{d\bar{I}_m}{d\bar{\tau}} \sim -\bar{I}_m,$$

from which we can deduce

$$\bar{I}_m \sim s_0 e^{-\bar{\tau}} + \frac{1}{\beta}\ln\left(\frac{s_0}{\sigma}\right) e^{-\bar{\tau}},$$

after matching with (B.11) as $\bar{\tau} \to 0$ and $\beta \to \infty$. By imposing $\bar{I}_m(T_\sigma) = \sigma$, we obtain the approximate value for the duration T_σ

$$T_\sigma \sim \left(1 + \frac{1}{\beta s_0}\right)\ln\left(\frac{s_0}{\sigma}\right), \tag{B.12}$$

as $\beta \to \infty$. We note for the parameter values used in Table 3, this approximation for T_σ yields $T_\sigma \approx 8.63$ (noting that "$s_0 = 1$" in this case), which is an acceptable approximation to $T_\sigma \approx 9.87$ given that $\beta = 4$ is only modestly large.

Appendix C. Expected time calculations for onset of epidemic

Described in this appendix are two formulations to estimate the expected time, $E(T_L)$, of the stochastic model to reach the onset of the epidemic. The first approximation, Section C.1, is an estimate calculated by adding the expected time for I_b to reach, for the first time, the pseudo-steady level $I_b^c = \mu(1-s_0)N/\gamma$ and the expected time for I_m to first reach σN given $I_b = I_b^c$; this approximation assumes that the uninfected population remains constant (i.e. $\approx N$) and involves the simple evaluation of two recurrence relations. The second approximation, Section C.2, uses a two variable recurrence relation, i.e. numbers of I_b and I_m, to determine the estimated time for $I_m = I_m^c = \sigma N$; once again the susceptible populations are assumed constant.

C.1. Simple formulation for $E(T_L)$

In this formulation we consider the rise of I_b and I_m as independent events and denote the population for $I_b = i = 0, 1, ..., I = I_b^c$ and $I_m = j = 0, 1, ..., J = I_m^c$. We assume that i and j are small compared to the total population N. We seek estimates for $E(T_1)$, the expected time for the first instance of $I_b = I_b^c$, and $E(T_2)$, the expected time for the first instance $I_m = I_m^c$ given that $I_b = I_b^c$, to find the total expected time for epidemic onset via $E(T_L) \approx E(T_1) + E(T_2)$. To calculate these expected times, we consider changes in population over discrete steps of fixed time interval δt, where the transition probabilities are given in Table 2. By defining E_i^b to be the expected number of discrete steps needed for $I_b = I_b^c$ given a starting point $I_b = i$ and E_j^m to be the expected number of steps for $I_m = I_m^c$ given $I_m = j$ (given $I_b = I_b^c$), then it follows that

$$E(T_1) \;=\; \delta t\, E_0^b, \qquad E(T_2) \;=\; \delta t\, E_0^m.$$

In the estimation of $E(T_1)$ we assume that the total uninfected population remains constant, so that those infected with non-mutant bird flu come from a fixed pool of size $(1 - s_0)N$. Let $p_u = \mu(1 - s_0)N\delta t$ be the probability of getting bird flu and $p_d = \gamma\, i\, \delta t$ be the probability of recovery, then the expected number of steps to $I_b = I_b^c$ satisfies the recurrence relation

$$E_i^b \;=\; 1 \;+\; p_u\, E_{i+1}^b \;+\; p_d\, E_{i-1}^b \;+\; (1 - p_d - p_u)\, E_i^b, \tag{C.1}$$

subject to $E_0^b \;=\; 1 \;+\; p_u\, E_1^b, + (1 - p_u)\, E_0^b$ and $E_I^b \;=\; 0$; this is illustrated in Figure 13. We note that the probability of mutation has been assumed negligible since $\varepsilon \ll \gamma$. The recurrence relation can be solved analytically, in which E_0^b can be expressed in terms of hypergeometric functions and a sum of Gamma functions, however, (C.1) can be more easily computed by writing $z_i = E_{i+1}^b - E_i^b$ for $i = 0, .., I - 1$, leading to two recurrence relations

$$z_i \;=\; \frac{p_d\, z_{i-1} - 1}{p_u}, \qquad E_i^b \;=\; E_{i+1}^b \;-\; z_i, \tag{C.2}$$

subject to $z_0 = -1/p_u$ and $E_I^b = 0$. Hence, by marching through the first recurrence relation for z_i to find z_{I-1} and then by marching back from $i = I - 1$ using the second recurrence relation to determine the desired value of $E(T_1) \approx \delta t\, E_0^b$.

To estimate $E(T_2)$ the procedure is the same. By assuming $I_b = I_b^c$, we approximate the transition probabilities as $p_u = (\varepsilon I_b^c + \beta\, j)\delta t$ (accounting for mutation and infection of the approximately fixed susceptible population N) and $p_d = \gamma\, j\, \delta t$ to obtain the same system as shown in equations C.1 and C.2, except i and E_i^b are swapped with j and E_j^m, respectively.

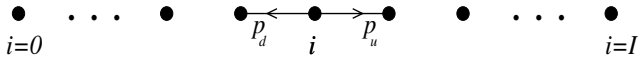

Figure 13: Figure showing the transition possibilities of $I_b = i$ bird flu infected individuals, where I represents the pseudo-steady population $I = I_b^c = \mu(1 - s_0)N/\gamma$.

C.2. Two variable formulation for $E(T_L)$

As can be seen in Figure 12, the simple formulation predicts the mean onset time T_L well for very small $\varepsilon = \mu$, but fails for larger, though still small, values of these parameters. An improved prediction can be made if we consider I_m and I_b simultaneously in the expected time formulation. We once again assume that S_n and S_b are constant, $s_0 N$ and $(1 - s_0)N$ respectively, and denote the infected populations with $I_b = i = 0, 1, ..., \rho I = \rho I_b^c$ and $I_m = j = 0, 1, ..., J = I_m^c$; where constant $\rho > 1$ is such that ρI_b^c is an assumed upper bound for the stochastic excursions of I_b about I_b^c (it is found that the estimated $E(T_L)$ remains relatively unchanged for any $\rho > 1.5$). Over a time-step δt, the population (i, j) can either remain unchanged or change in one of five directions with probabilities $p_1, ..., p_5$; the transition probabilities being shown in Table 4 and illustrated in Figure 14.

For the two-variable formulation, we let

$$E_{i,j} = E(\text{number of steps for } I_m = I_m^c \,|\, I_b = i, I_m = j),$$

whereby, an approximation to the epidemic onset time is given by $E(T_L) \approx \delta t \, E_{0,0}$, i.e. the expected time taken for the first instance of $I_m = J = \sigma N$ starting from zero infected individuals at $t = 0$. It follows from the transitional probabilities in Table 4, that $E_{i,j}$ is given by the recurrence relation

$$E_{i,j} = 1 + p_1 E_{i,j+1} + p_2 E_{i+1,j} + p_3 E_{i,j-1} + p_4 E_{i-1,j} + p_5 E_{i-1,j+1} + \left(1 - \sum_{k=1}^{5} p_k\right) E_{i,j},$$

which can be rewritten as

$$\begin{aligned} p_1 \left(E_{i,j+1} - E_{i,j}\right) \,+\, p_2 \left(E_{i+1,j} - E_{i,j}\right) \,+\, p_3 \left(E_{i,j-1} - E_{i,j}\right) & \\ + p_4 \left(E_{i-1,j} - E_{i,j}\right) \,+\, p_5 \left(E_{i-1,j+1} - E_{i,j}\right) \;&=\; -1, \end{aligned} \tag{C.3}$$

and are subject to

$$\left.\begin{array}{ll} i \,=\, 0 & \text{Eqn. (C.3) with } \; p_4 \,=\, p_5 \,=\, 0, \\ i \,=\, \rho\, I & \text{Eqn. (C.3) with } \; p_2 \,=\, 0, \\ j \,=\, 0 & \text{Eqn. (C.3) with } \; p_3 \,=\, 0, \\ j \,=\, J & E_{i,J} \;=\; 0. \end{array}\right\} \tag{C.4}$$

Equations (C.3) and boundary conditions (C.4) form a closed, sparse linear system for $(\rho I + 1) \times J = \rho\sigma\mu(1 - s_0)N^2/\gamma + \sigma N$ unknown variables.

Despite the sparseness of the matrix, for large N this is a computationally massive problem, for example, in the $\mu = \varepsilon = 0.1$ case shown in Figure 12 the number of variables $E_{i,j}$ is around 2×10^9. An alternative approach that leads to a good approximation to $E_{0,0}$, but using significantly less computation, involves converting (C.4) into a partial differential equation employing asymptotic expansions as $N \to \infty$. Let $x = i\gamma/\rho\mu(1 - s_0)N = i/\rho I_b^c$, $y = j/\sigma N =$

(I_b, I_m) at time t	(I_b, I_m) at time $t + \delta t$	Transitional probability
(i, j)	$(i, j+1)$	$p_1 = \beta\, j\, \delta t$
(i, j)	$(i+1, j)$	$p_2 = \mu\,(1 - s_0) N\, \delta t$
(i, j)	$(i, j-1)$	$p_3 = \gamma\, j\, \delta t$
(i, j)	$(i-1, j)$	$p_4 = \gamma\, i\, \delta t$
(i, j)	$(i-1, j+1)$	$p_5 = ((\beta/N)\, i\, j + \varepsilon\, i)\, \delta t$
(i, j)	(i, j)	$1 - \sum_{k=1}^{5} p_k$

Table 4: Possible state changes of $(I_b, I_m) = (i, j)$ with associated transitional probabilities. They correspond to those shown in Table 2, except that $(S_n, S_b) = (s_0 N, (1 - s_0)N)$.

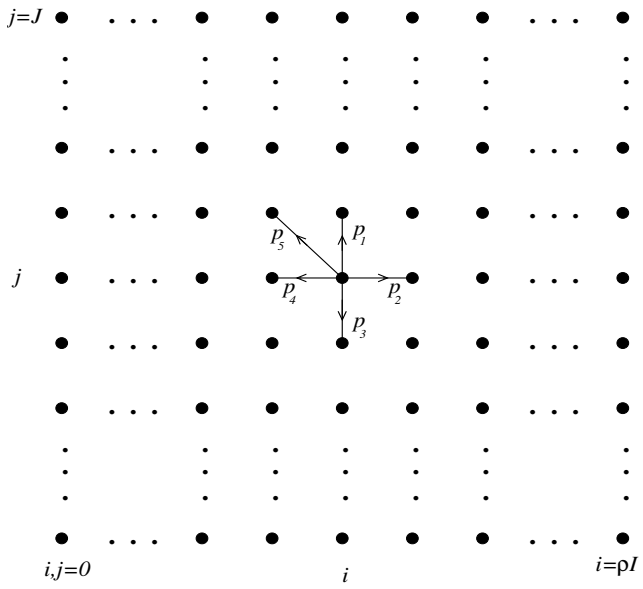

Figure 14: Schematic of the transitions presented in Table 4 and showing the boundaries of variables $(I_b, I_m) = (i, j)$, where $J = I_m^c = \sigma N$, $I = I_b^c = \mu(1 - s_0)N/\gamma$ and constant $\rho > 1$.

j/I_m^c and $E(x, y) = E_{i,j}\delta t$ (so that $E(T_L) \approx E(0, 0)$), then taking Taylor expansions up to and including terms of size $O(1/N)$ we obtain as $N \to \infty$,

$$A_1 \frac{\partial^2 E}{\partial x^2} + A_2 \frac{\partial^2 E}{\partial x \partial y} + A_3 \frac{\partial^2 E}{\partial y^2} + B_1 \frac{\partial E}{\partial x} + B_2 \frac{\partial E}{\partial y} = 1, \tag{C.5}$$

defined on $x \in (0, 1)$ and $y \in (0, 1)$, where

$$A_1 = -\frac{\gamma(\varepsilon\rho x + \gamma(1 + \rho x) + \rho\sigma\beta xy)}{2\mu s_0 N \rho^2}, \quad A_2 = \frac{\varepsilon x + \sigma\beta y}{\sigma N},$$
$$A_3 = -\frac{\gamma\sigma y(\beta + \gamma) + \mu\rho s_0 x(\varepsilon + \beta\sigma y)}{2\gamma N \sigma^2},$$
$$B_1 = \varepsilon x - \frac{\gamma}{\rho}(1 - \rho x) + \sigma\beta xy \quad B_2 = -y(\beta - \gamma) - \frac{\mu\rho s_0 x(\varepsilon + \beta\sigma y)}{\gamma\sigma},$$

with $\hat{\beta} = \beta N/\gamma$, subject to

$$\frac{\partial E}{\partial x}(0,y) = -\frac{1}{\gamma}, \quad \frac{\partial E}{\partial x}(1,y) = \frac{1}{\gamma+\varepsilon}, \quad \frac{\partial E}{\partial y}(x,0) = -\frac{\sigma\gamma}{\varepsilon\mu(1-s_0)}, \quad E(x,1) = 0. \tag{C.6}$$

Here, the Neumann conditions result from the leading order gradients normal to the sides of the domain as $N \to \infty$. The results were found to be sensitive to the choice of boundary conditions, but these yielded solutions that agree well with the mean of the stochastic simulations.

The system (C.5) and (C.6) is solved using a finite element scheme on a non-uniform rectangular grid. The solutions shown in Figure 12 were generated on a grid with fixed interval $dx = 1/\rho I_b^c$ in the x direction and in the y direction we used $dy = 1/I_m^c, 10/I_m^c$ and $100/I_m^c$ in the regions $y \in [0, 0.01], [0.01, 0.1]$ and $[0.1, 1]$, respectively. The changing steps in y reflect the presence of a boundary layer around $y = 0$, whilst $\partial E/\partial y = O(1)$ in $(0, 1]$. We note that the dx and smallest dy steps are equivalent to solving the original recurrence relation, however, for the example stated above the number of values for $E(x_i, y_j)$ to be determined is reduced to around 2×10^7. We further note that for a good approximation, a fixed dx at the stated value was needed.